Mixed-component metal-organic frameworks (MC-MOFs): enhancing functionality through solid solution formation and surface modifications

Andrew D. Burrows

Department of Chemistry, University of Bath, Claverton Down, Bath BA2 7AY, UK. E-mail: a.d.burrows@bath.ac.uk.

Abstract

Mixed-component metal-organic frameworks (MC-MOFs) are metal-organic frameworks that have different linkers or metals with the same structural role. Many of these mixed-ligand or mixed-metal MOFs are solid solutions, in which the proportions of the ligands or metals can be adjusted or even controlled. These MC-MOFs can be prepared directly, using more than one metal or ligand in the synthesis, or formed by post-synthetic modification. A second class of MC-MOFs have core-shell structures, and these can be prepared through epitaxial growth of one MOF on the surface or another or post-synthetic modification of the crystal surfaces. This review describes the syntheses, structures and properties of mixed-ligand, mixed-metal and core-shell MOFs, and highlights some of the potential benefits in functionality that these materials have.

1. Introduction

Over the past ten years, the study of materials in which bridging ligands connect metal centres or aggregates into extended coordination networks has become a major area of chemistry.[1-5] Many of these materials exhibit porosity, and applications such as hydrogen storage,[6] separations,[7] and catalysis[8] are attracting considerable attention.

Perhaps inevitably for such a fast-growing and interdisciplinary area, there is currently a lack of consensus on the best terms to describe these new materials. To some, they are coordination polymers, whereas to others they are metal-organic frameworks (MOFs), though a number of other names are also in usage. Some workers, notably Yaghi, have sought to distinguish between coordination polymers and MOFs on the basis of bond strength.[9] Others, notably Robson, have argued that this distinction is unnecessary.[3] The term metal-organic framework has become so ubiquitous that it is difficult to avoid, and in this review the term is used throughout to describe coordination network structures, regardless of the ligands employed.

This review concerns the formation of MOFs containing either mixed ligands, or mixed metals. For the materials under consideration, the different ligands (or metals) employed have similar structural roles within the MOF, thus allowing access to solid solutions in which the relative proportions of the ligands (or metals) can be adjusted. The term 'solid solution' is used somewhat lightly, as in some cases a completely random arrangement of ligands or metals may not be present. Mixed-ligand MOFs are described in Section 2, and mixed-metal MOFs are described in Section 3.

The other type of material that will be examined are MOFs which adopt 'core-shell' structures, in which the outside of a MOF crystal is chemically different from the centre. Such systems can be formed through epitaxial growth, in which a MOF is grown onto the surface of another, or *via* post-synthetic modification of the MOF surface. These materials are described in Section 4.

Different groups have used differing terminology to describe the types of MOF considered in this review. For example, mixed-ligand MOFs have been termed MIXMOFs by Baiker,[10] multivariate MOFs (MTV-MOFs) by Yaghi[11] and coordination co-polymers by Matzger.[12] We introduce the term mixed-component MOFs (MC-MOFs) as an over-arching term for all of the mixed-ligand and mixed-metal MOFs described in this review, and summarise the categories in Figure 1.

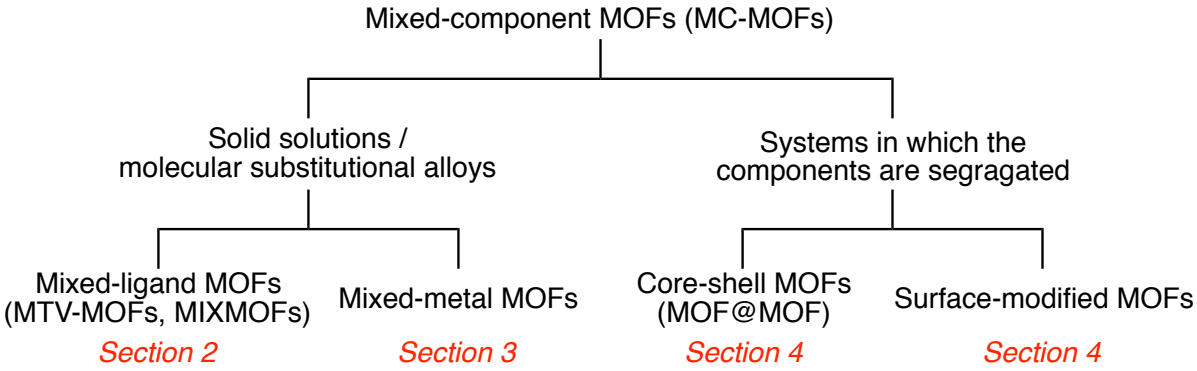

Figure 1. The different categories of mixed-component MOFs, and where they are discussed in this Highlight article.

Before looking in detail at examples of MC-MOFs, it is important to stress that this term does not encompass all mixed-ligand or mixed-metal MOFs. The compounds $[Zn_2(bdc)_2(dabco)]$ **1** (bdc = 1,4-benzenedicarboxylate, dabco = 1,4-diazabicyclo[2.2.2]octane),[13] shown in Figure 2, and $[Zn_4O(bdc)(btb)_{4/3}]$ **2** (UMCM-1, btb = 1,3,5-benzenetribenzoate)[14] are both mixed-ligand MOFs in which the two types of bridging ligand have different structural roles. As a consequence, their proportions are not free to be altered, and they are not MC-MOFs, though, in the case of **2**, the ratio of ligands used in the synthesis is crucial in the formation of **2** as opposed to MOFs containing just bdc or btc.[15] Mixed-metal MOFs can be assembled in a stepwise manner through use of metalloligands. For example, $[Al(dppd)_3]$ **3** (dppd = 1,3-di(4-pyridyl)propane-1,3-dionate) reacts with $AgNO_3$ to form $[Al(dppdAg)_3](NO_3)_3$ **4** in which the silver(I) centres link molecules of **3** together into a three-dimensional network.[16] Since the aluminium and silver atoms have different structural roles in **4**, it is not a MC-MOF. Even using two metal salts in a one-pot reaction does not guarantee formation of a MC-MOF. Caskey and Matzger used the reaction of a mixture of zinc(II) nitrate and cobalt(II) nitrate with H_3btc (btc = 1,3,5-benzenetricarboxylate) to form $[ZnCo(btc)(NO_3)(EtOH)_3]$ **5**, a mixed-metal analogue of $[Zn_2(btc)(NO_3)(EtOH)_3]$ **6** (MOF-4).[17] In **5**, the zinc and cobalt centres have different coordination geometries, with the zinc centres tetrahedral and the cobalt centres octahedral. This is therefore not a MC-MOF.

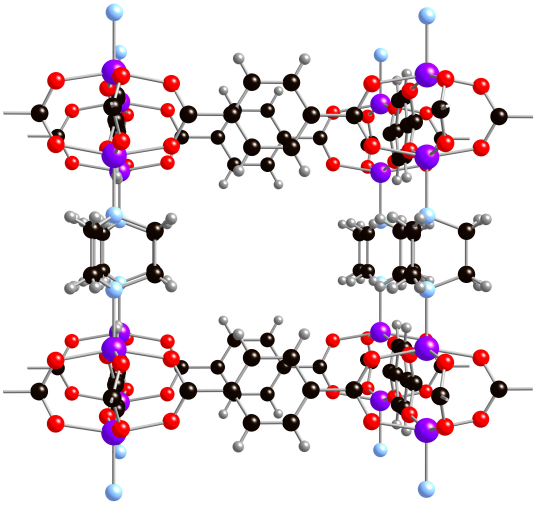

Figure 2. Part of the structure of $[Zn_2(bdc)_2(dabco)]$ **1**, with zinc atoms purple, oxygen atoms red, nitrogen atoms blue, carbon atoms black and hydrogen atoms grey.

Why might MC-MOFs be of interest? One of the key characteristics of these materials is the ability to vary the proportions of the ligands or metals in the MOF, which provides the potential to control pore sizes and compositions, and hence tailor properties. Mixed-ligand and mixed-metal MOFs can be considered as *molecular substitutional alloys*, and as such they might be expected to follow Vegard's Law. This is an empirical rule which holds that, at a given temperature, there is a linear relationship between the crystal lattice parameters of an alloy and the concentrations of the constituent elements. For MC-MOFs, the rule will hold if the unit cell dimensions depend linearly on the concentrations of the metal ions or ligands that are being substituted.

This review describes the structures and properties of MC-MOFs that have been prepared to date, with the aim of demonstrating some of the enormous potential that these materials have.

2. Mixed-linker MOFs

One way of introducing multiple functionalities into the pores of a MOF is to use more than one type of linker in the synthesis. Provided that these linkers have similar lengths, donor groups and solubilities, they might be expected to be incorporated in an equivalent manner into the MOF product, giving a single phase MC-MOF with the linkers included in random positions, as opposed to a mixture of single-linker MOFs. This is shown schematically in Figure 3.

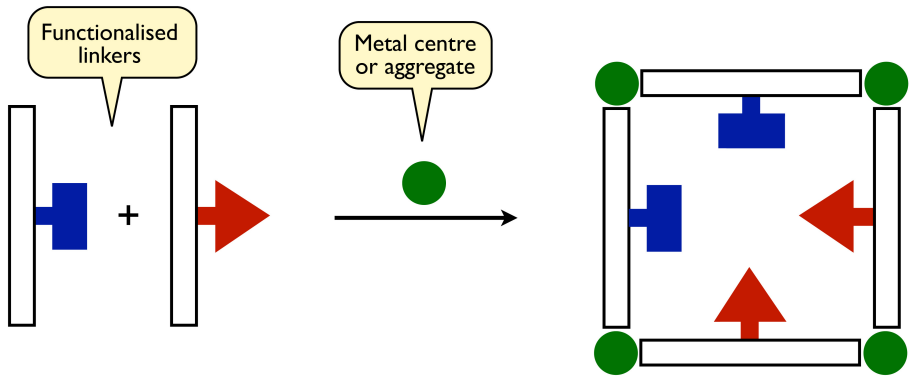

Figure 3. Schematic representation of the formation of a mixed-ligand MOF by using isosteric ligands with different substituents in the synthesis.

2.1 MC-MOFs containing more than one dicarboxylate linker

Most examples of the multiple-linker approach to MC-MOFs have used dicarboxylate ligands. The first example was described by Kim and co-workers,[18] who used a 1:1 mixture of H_2bdc and H_2tmbdc (tmbdc = 2,3,5,6-tetramethyl-1,4-benzenedicarboxylate) together with zinc(II) and dabco to form $[Zn_2(bdc)(tmbdc)(dabco)]$ **7**. Compound **7** is isomorphous with $[Zn_2(bdc)_2(dabco)]$ **1** (Figure 2) and $[Zn_2(tmbdc)_2(dabco)]$ **8**, with the bdc and tmbdc ligands disordered in the crystal structure. The nitrogen sorption isotherms show that the surface area of **7** lies between the values measured for **1** and **8**. However, the smaller pores formed with tmbdc are more favourable for H_2 adsorption, and as a consequence **7** was shown to adsorb a greater amount of hydrogen (in $cm^3\ g^{-1}$) than either **1** or **8**.

Burrows and co-workers showed that the mixed-dicarboxylate approach could be applied to longer ligands.[19] The reaction between zinc(II) nitrate and a mixture of the aldehyde-tagged diacid H_2bpdc-CHO and the methoxy-tagged diacid H_2bpdc-OMe generated $[Zn_4O(bpdc\text{-}CHO)_{0.3}(bpdc\text{-}OMe)_{2.7}]$ **9**. Notably, the two dicarboxylate linkers were unequally included into the MC-MOF, with a 1:1 mixture of H_2bpdc-CHO and H_2bpdc-OMe in the reaction mixture leading to incorporation of the linkers in the ratio 1:9.

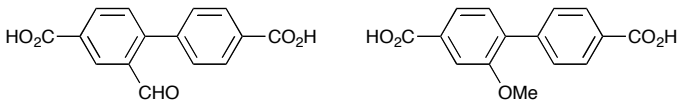

H_2bpdc-CHO H_2bpdc-OMe

The IRMOF system of general formula $[Zn_4OL_3]$ has attracted the most attention to date in studies of mixed-carboxylate MOFs, and the structure of $[Zn_4O(bdc\text{-}NH_2)_3]$ **10** (IRMOF-3, bdc-NH_2 = 2-amino-1,4-benzenedicarboxylate) is shown in Figure 4. The groups of Baiker, Matzger and Yaghi have all studied the formation of mixed-ligand zinc(II) MOFs with the same structural architecture as $[Zn_4O(bdc)_3]$ **11** (MOF-5) and IRMOF-3, formed with mixtures of bdc and bdc-NH_2. Baiker and co-workers prepared $[Zn_4O(bdc)_{3-x}(bdc\text{-}NH_2)_x]$ **12** with $x \leq 1.2$, but found that higher proportions of bdc-NH_2 led to the presence of more than one phase in the product.[10] They assessed the mixed-ligand MOFs as heterogeneous catalysts in the reaction between propylene oxide and carbon dioxide to form propylene carbonate, and

demonstrated a correlation between the catalyst activity and the number of amino groups present. Amino groups have also been shown to facilitate the adsorption of palladium from $Pd(OAc)_2$.[20] As a consequence, $[Zn_4O(bdc)_{2.7}(bdc\text{-}NH_2)_{0.3}]$ **12a** adsorbs more palladium than $[Zn_4O(bdc)_{2.85}(bdc\text{-}NH_2)_{0.15}]$ **12b**. Moreover, the catalytic activity of the resultant Pd-modified materials for the oxidation of CO was shown to depend upon the amount of Pd present, so increasing the proportion of bdc-NH_2 in the MOF led to a more active catalyst following Pd-modification.

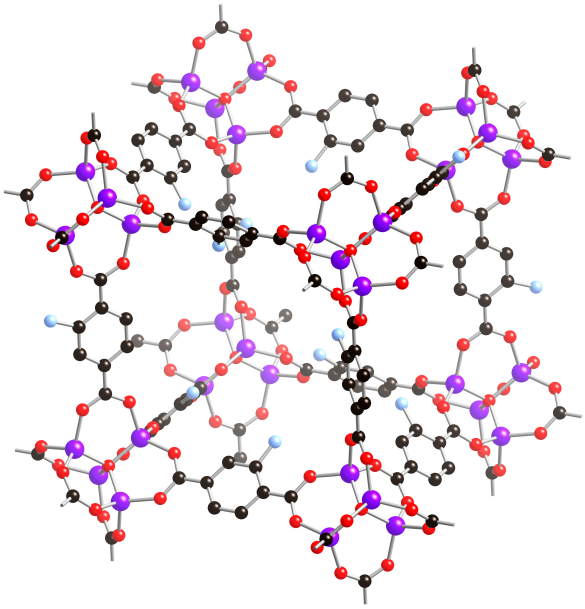

Figure 4. Part of the structure of $[Zn_4O(bdc\text{-}NH_2)_3]$ **10** (IRMOF-3), with zinc atoms purple, oxygen atoms red, nitrogen atoms blue and carbon atoms black. Hydrogen atoms have been omitted for clarity. The amino groups are disordered, and only one position per linker is shown.

Matzger and co-workers studied the $[Zn_4O(bdc)_{3-x}(bdc\text{-}NH_2)_x]$ (**12**) system, largely in comparison to core-shell materials which are described in Section 4.2.[12] NMR analysis of the digested $[Zn_4O(bdc)_{3-x}(bdc\text{-}NH_2)_x]$ samples suggested the degree of incorporation of the two linkers was approximately equivalent to the mole fractions employed in the synthesis. They also demonstrated that the BET surface areas of the products, calculated from N_2 adsorption measurements, decreased in an approximately linear manner with increasing proportion of bdc-NH_2, from the value of 3170 $m^2\ g^{-1}$ for **11** (MOF-5) to that 2660 $m^2\ g^{-1}$ for **10** (IRMOF-3).

Yaghi and co-workers have recently published an extensive account of mixed-dicarboxylate MOFs based on the IRMOF system.[11] They made MOFs containing bdc and one or more of the functionalised dicarboxylates bdc-NH_2, 2-bromo-1,4-benzenedicarboxylate (bdc-Br), 2,5-dichloro-1,4-benzenedicarboxylate (bdc-Cl_2), 2-nitro-1,4-benzenedicarboxylate (bdc-NO_2), 2,5-dimethyl-1,4-benzenedicarboxylate (bdc-Me_2), 1,4-naphthalenedicarboxylate (1,4-ndc), 2,5-bis(allyloxy)-1,4-benzenedicarboxylate (bdc-$(OAl)_2$) and 2,5-bis(benzyloxy)-1,4-benzenedicarboxylate (bdc-$(OBz)_2$), denoting the products as multivariate (MTV) MOFs.

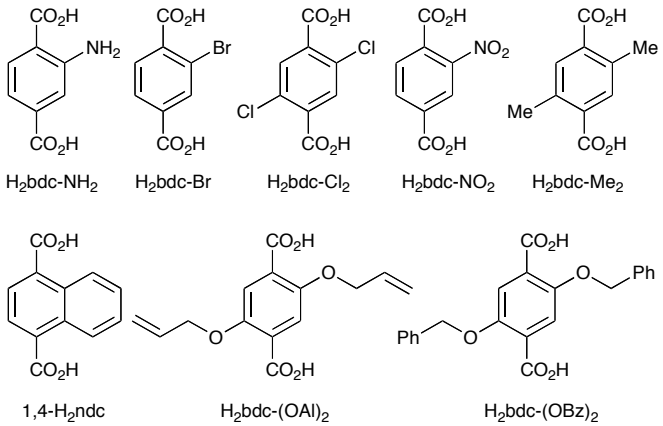

As part of their study, they prepared $[Zn_4O(bdc)_{2.14}(bdc\text{-}NO_2)_{0.86}]$ **13**, demonstrating that bdc-NO_2 could be incorporated into the MOF-5 structure, despite the fact that this ligand does not form $[Zn_4O(bdc\text{-}NO_2)_3]$ on reaction with zinc(II) nitrate when used as the only dicarboxylate ligand. They also demonstrated that the proportions of the linkers present in the MTV-MOFs were not the same as those used in the syntheses. For example, when $Zn(NO_3)_2{\cdot}4H_2O$ was reacted in DMF with equimolar amounts of H_2bdc, H_2bdc-NH_2, H_2bdc-Br and H_2bdc-Cl_2, the product was characterised as $[Zn_4O(bdc)_{1.44}(bdc\text{-}NH_2)_{0.17}(bdc\text{-}Br)_{0.81}(bdc\text{-}Cl_2)_{0.58}]$ **14**, with the relative proportions of the four ligands 1 : 0.12 : 0.56 : 0.40. In the synthesis of $[Zn_4O(bdc)_{0.70}(bdc\text{-}NH_2)_{0.10}(bdc\text{-}Br)_{0.39}(bdc\text{-}NO_2)_{0.20}(bdc\text{-}Me_2)_{0.47}(ndc)_{0.39}\{bdc\text{-}(OAl)_2\}_{0.34}\{bdc\text{-}(OBz)_2\}_{0.39}]$ **15**, they showed that as many as eight different dicarboxylates could be incorporated into a single MOF structure.

Perhaps the most intriguing aspect of Yaghi's report was their demonstration that the properties of the mixed dicarboxylate MOFs are not simply linear combinations of the constituents. Hydrogen isotherms show that $[Zn_4O(bdc)_{1.52}\{bdc\text{-}(OAl)_2\}_{0.73}\{bdc\text{-}(OBz)_2\}_{0.76}]$ **16** has a greater H_2 uptake capacity than $[Zn_4O(bdc)_{2.05}\{bdc\text{-}(OAl)_2\}_{0.95}]$ **17**, $[Zn_4O(bdc)_{2.14}\{bdc\text{-}(OBz)_2\}_{0.86}]$ **18** or MOF-5. In addition, $[Zn_4O(bdc\text{-}NO_2)_{0.74}\{bdc\text{-}(OAl)_2\}_{1.06}\{bdc\text{-}(OBz)_2\}_{1.20}]$ **19** has over 400 % better selectivity for CO_2 over CO than MOF-5. These results suggest the possible presence of particular sequences of linkers within the MOF frameworks, which in turn implies that these materials may not be simple solid solutions that contain a random distribution of linkers. However, no data on the ordering of ligands in these systems is yet available.

Kitagawa and co-workers have prepared the compounds [Zn(1,3-bdc-NO_2)(4,4'-bipy)] (**20**, 1,3-bdc-NO_2 = 5-nitro-1,3-benzenedicarboxylate) and [Zn(1,3-bdc-OMe)(4,4'-bipy)] (**21**, 1,3-bdc-OMe = 5-methoxy-1,3-benzenedicarboxylate), both of which contain interdigitated two-dimensional layers, one of which for **20** is shown in Figure 5.[21] Although the two compounds have very similar cell parameters, they behave differently on activation. In **20**, there is a reorganisation of the interdigitation on solvent removal, giving rise to a non-porous structure. In contrast, **21** showed a much smaller structural change on activation, and is porous. Use of a 1:1 ratio of 1,3-H_2bdc-NO_2 and 1,3-H_2bdc-OMe in the synthesis gave the compound $[Zn(1,3\text{-}bdc\text{-}NO_2)_{0.48}(1,3\text{-}bdc\text{-}OMe)_{0.52}(4,4'\text{-}bipy)]$ **22a**, and use of other ligand ratios also showed a slight propensity for incorporation of 1,3-bdc-OMe in preference to 1,3-bdc-NO_2.

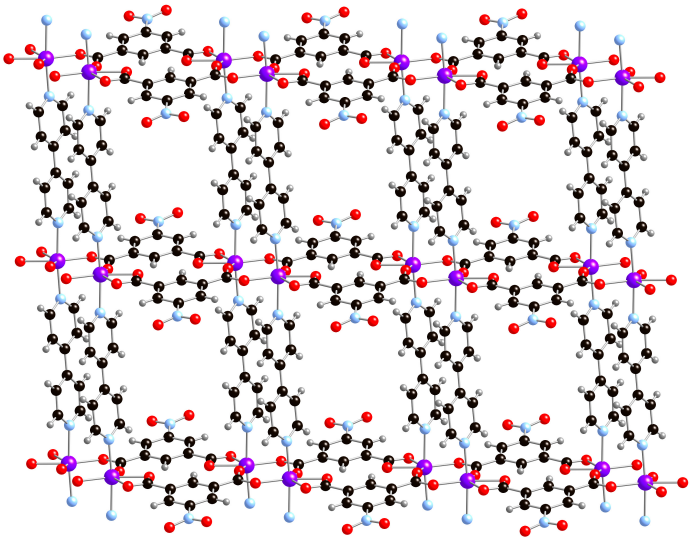

Figure 5. Part of the sheet structure of [Zn(1,3-bdc-NO_2)(4,4'-bipy)] **20**, with zinc atoms purple, oxygen atoms red, nitrogen atoms blue, carbon atoms black and hydrogen atoms grey.

The difference in structural behaviour on activation between **20** and **21** leads to contrasting gas adsorption properties. Compound **20** exhibited gate-opening sorption for both H_2O and CO_2, whereas **21** showed linear uptake of H_2O and Type I isotherms for CO_2. The mixed-ligand compounds displayed adsorption properties that have features in common with both parent compounds **20** and **21**. For example, **20** selectively adsorbed CO_2 from a CH_4/CO_2 mixture but with negligible uptake (2.5 $dm^3\ g^{-1}$), whereas **21** adsorbed considerably more CO_2 than **20** (40 $dm^3\ g^{-1}$), but also adsorbed some CH_4. The mixed-ligand compound [Zn(1,3-bdc-NO_2)$_{0.13}$(1,3-bdc-OMe)$_{0.87}$(4,4'-bipy)] **22b** adsorbed almost as much CO_2 as **21** (30 $dm^3\ g^{-1}$), but did not adsorb CH_4 at all. Thus **22b** contains the advantages of both **20** and **21** in a single material.

Lin and co-workers used mixtures of bdc and bdc-NH_2 to prepare amino-tagged versions of [$Fe_3O(Cl)(H_2O)_2(bdc)_3$] **23** (MIL-101(Fe)).[22] Powder X-ray diffraction studies showed that compounds isostructural with **23** were only formed with a mole fraction of bdc-NH_2 of up to 17.5 %. Any higher, and the product adopted a different structure. The proportion of bdc-NH_2 incorporated into the product was, in most cases, slightly higher than the ratio in the reaction mixture.

Kleist, Baiker and co-workers showed that mixed-linker MOFs can be prepared in the MIL-53 system.[23] The structure of [Al(OH)(bdc)] **24** (MIL-53(Al)) is shown in Figure 6. By reacting aluminium nitrate with combinations of H_2bdc and H_2bdc-NH_2, the MOFs [Al(OH)(bdc)$_{1-x}$(bdc-NH_2)$_x$] **25** (x = 0.1, 0.5, 0.9) were formed, and were shown to be all single-phase materials. The increasing presence of bdc-NH_2 was monitored by IR and solid-state NMR spectroscopy in addition to powder X-ray diffraction.

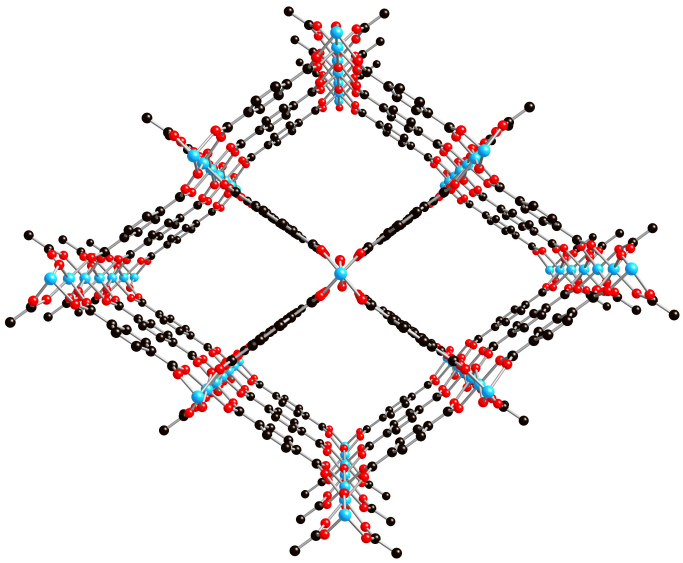

Figure 6. Part of the structure of [Al(OH)(bdc)] **24**, with aluminium atoms blue, oxygen atoms red and carbon atoms black. Hydrogen atoms have been omitted for clarity.

2.2 MC-MOFs based on non-dicarboxylate ligands

Yaghi and co-workers have reported a wide range of network structures containing imidazolate ligands. These materials are often referred to as zeolitic imidazolate frameworks (ZIFs) because of the similarity of the angle between the nitrogen lone pairs in the imidazolate ligand to the Si–O–Si angle in zeolites (~145°), which leads to parallels between the structures of ZIFs and zeolites.[24] The compounds typically contain tetrahedral metal centres that are connected to four linkers. Using a high-throughput approach, they prepared a number of examples of ZIFs containing two different imidazolates or imidazolate-like ligands.[25, 26] In the majority of these structures, the two ligands adopt different positions in the structure. For example, [Zn(bim)(nim)] **26** (ZIF-68, bim = benzimidazolate, nim = 2-nitroimidazolate) has the gmelinite structure with the phenyl rings of the bim ligands directed into hexagonal channels, as shown in Figure 7.

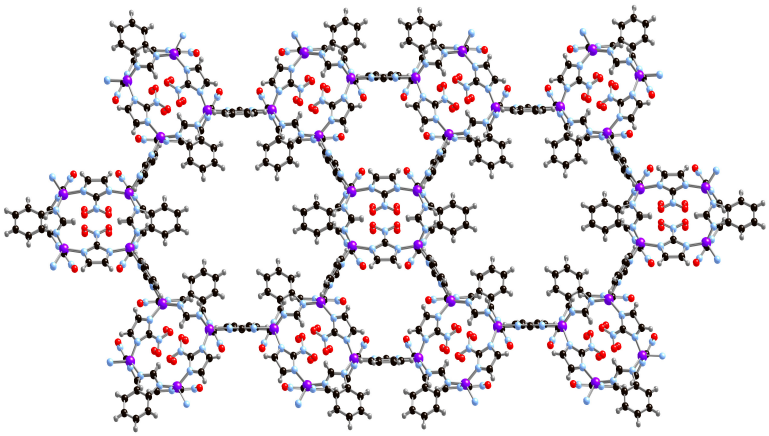

Figure 7. Part of the structure of [Zn(bim)(nim)] **26** (ZIF-68), with zinc atoms purple, oxygen atoms red, nitrogen atoms blue, carbon atoms black and hydrogen atoms grey.

There are, however, several examples of ZIFs that can be classified as MC-MOFs due to the presence of disorder between the linkers. In the compounds $[Zn(im)_{1.81}(bim)_{0.19}]$ **27** (ZIF-62), $[Zn(im)_{1.13}(nim)_{0.87}]$ **28** (ZIF-70), $[Zn(nim)_{1.74}(dmbim)_{0.26}]$ **29** (ZIF-73) and $[Zn(im)_{1.5}(cbim)_{0.5}]$ **30** (ZIF-76)] (im = imidazolate, dmbim = 5,6-dimethylbenzimidazolate, cbim = 5-chlorobenzimidazolate) some of the ligands are ordered (generally the smaller one, which is present as the major component), whereas others are disordered. For example, in **27**, three of the four crystallographically independent linkers are imidazolate, whereas the fourth is disordered between imidazolate (62.5 %) and benzimidazolate (37.5 %).

The presence of the two different ligands can have an important effect on the type of network adopted. For example, neither $[Zn(im)_2]$ nor $[Zn(nim)_2]$ form the gmelinite network, whereas this is the structure adopted by **28**, demonstrating that use of mixed ligands in a synthesis can afford access to structural types that are otherwise unavailable with those ligands. Compound **28** was shown to have a Langmuir surface area of 1970 $m^2\ g^{-1}$, and displayed excellent selectivity for adsorption of CO_2 over CO.

Feng and co-workers have also prepared mixed-ligand ZIFs. They prepared $[Zn(im)_{2-x}(mbim)_x]$ (mbim = 5-methylbenzimidazolate) **31** and showed that the structure adopted depends on the ratio of benzene and 2-amino-1-butanol solvents used in the reaction.[27]

2.3 MC-MOFs with different ligand oxidation levels

Theoretical and experimental studies have shown that inclusion of alkali metal centres into MOFs can enhance their H_2 adsorption properties.[28] With this in mind, Hupp and co-workers prepared $[Zn_2(2,6\text{-ndc})_2(dpn)]$ **32** (2,6-ndc = 2,6-naphthalenedicarboxylate, dpn = *N*,*N*′-di(pyridyl)-1,4,5,8-naphthalenetetracarboxydiimide)[29, 30] and $[Zn_2(2,6\text{-ndc})_2(dpt)]$ **33** (dpt = di-3,6-(4-pyridyl)-1,2,4,5-tetrazine),[31] both of which contain reducible pillaring ligands. Compounds **32** and **33** are structurally similar to **1**, containing Zn-dicarboxylate layers that are connected into a three-dimensional structure by the *N,N*′-donor ligands, though **33** is triply-interpenetrated, whereas both **1** and **32** are doubly-interpenetrated.

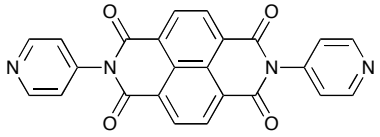

dpn

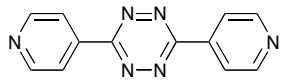

dpt

On treatment with lithium, sodium or potassium naphthalenide, the dpn or dpt linkers in **32** and **33** were partially reduced, giving MOFs that formally contain both the neutral linker and its monoanion, with the charges balanced by the included Group 1 cations. The most promising materials for H_2 adsorption were those in which the cation incorporation was low. For example, the H_2 uptake in $Na_{0.24}[Zn_2(2,6\text{-ndc})_2(dpt)]$ **34** was enhanced by 43 % over that for **33**. The reduction appears to affect adsorption by favourable displacement of the interpenetrated frameworks with the alkali metal cations not themselves readily available as adsorption sites.

2.4 MC-MOFs formed via post-synthetic modification of the bridging ligands

Post-synthetic modification is the process by which a pre-formed MOF undergoes a solid-state reaction to convert it into another MOF. Although not exclusive to organic transformations, many examples of post-synthetic modification involve functional group interconversions on the bridging ligands. If a post-synthetic modification reaction does not go to completion, it will result in a mixed-ligand MOF, as shown schematically in Figure 8. The use of post-synthetic modification in MOF chemistry has recently been reviewed,[32] and only examples giving mixed-ligand MOFs are described here.

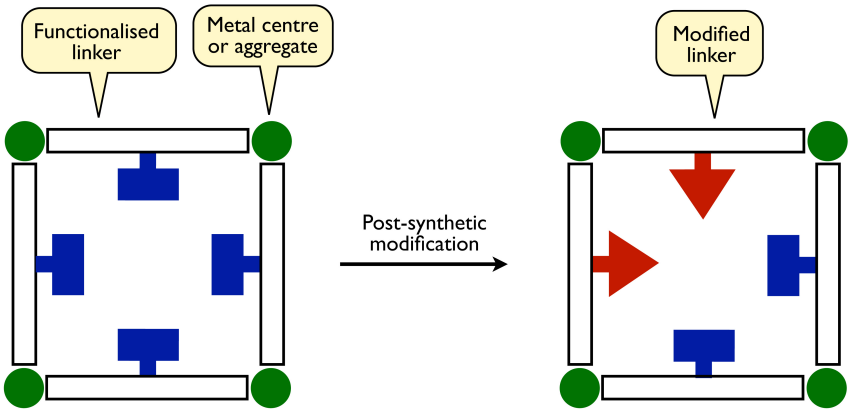

Figure 8. Schematic representation of how post-synthetic modification can be used to generate a mixed-ligand MC-MOF.

The most common ligand used in post-synthetic modification studies to date has been 2-amino-1,4-benzenedicarboxylate (bdc-NH_2). Not only is H_2bdc-NH_2 readily available, but the amine group can undergo a wide variety of transformation reactions. The first report of post-synthetic modification on [Zn_4O(bdc-NH_2)$_3$] **10** (IRMOF-3) was published by Cohen and Wang in 2007.[33] They showed that when **10** was treated with acetic anhydride, acylation of the amine groups occurred with 80% conversion after 5 days to give [Zn_4O(bdc-NH_2)$_{0.6}${bdc-NHC(O)Me}$_{2.4}$] **35**.

Further studies with a range of linear alkyl anhydrides revealed that the extent of modification could be increased by changing the reaction conditions, but that it decreased with increasing alkyl chain length. Thus, for example, O{C(O)$(CH_2)_n$Me}$_2$ gave virtually complete reaction for $n \leq 4$, though this decreased to 81 % for $n = 6$ and to 31 % for $n = 12$.[34] This can be rationalised using steric arguments, since the introduction of bulky groups blocks pores and channels, thus restricting access of the reagent to the unmodified groups.

Cohen and co-workers have also demonstrated that tandem reactions are possible.[35] Reaction of **10** with crotonic anhydride was undertaken to give complete functionalisation of the amine groups, forming [Zn_4O{bdc-NHC(O)CH=CHMe}$_3$] **36**. Further reaction of **36** with bromine was used to form the mixed-ligand MOFs [Zn_4O{bdc-NHC(O)CH=CHMe}$_{3-x}${bdc-NHC(O)CHBrCHBrMe}$_x$] **37**, with the reaction time used to control the degree of bromination. Incomplete post-synthetic modification opens up the possibility of a second kind of tandem reaction, in which the unmodified groups from the first reaction are modified in a second reaction. This was illustrated by the reaction of **10** with crotonic anhydride for shorter periods of time than that used to form **36** followed by reaction of the remaining amine

groups on the incompletely modified MOFs with acetic anhydride to give $[Zn_4O\{bdc\text{-}NHC(O)CH{=}CHMe\}_{3-x}\{bdc\text{-}NHC(O)Me\}_x]$ **38** (Scheme 1).

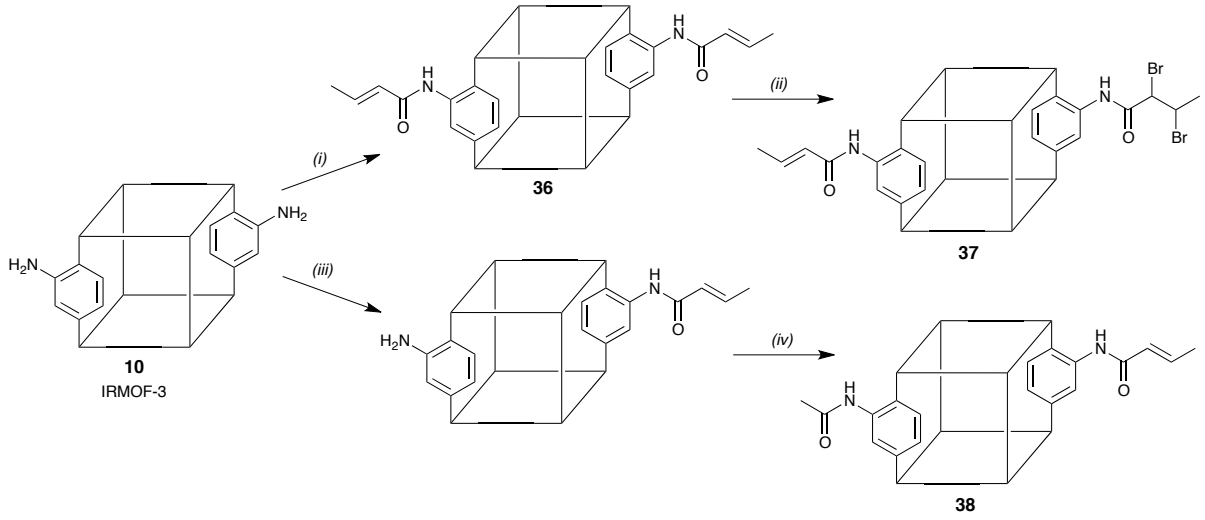

Scheme 1 *(i)* $O\{C(O)CH{=}CHMe\}_2$, $CHCl_3$, 1 day; *(ii)* Br_2, $CHCl_3$; *(iii)* $O\{C(O)CH{=}CHMe\}_2$, $CHCl_3$, 7 days; *(iv)* $O\{C(O)Me\}_2$, $CHCl_3$.

Reaction of **10** with benzoic anhydride gave $[Zn_4O(bdc\text{-}NH_2)_{3-x}\{bdc\text{-}NHC(O)Ph\}_x]$ **39**, in which x can be controlled by variation of the reaction time or the concentration.[36] The modified materials showed higher gravimetric uptake of H_2 than IRMOF-3 due to interactions between the adsorbed H_2 and the phenyl substituents on the amide groups. Surprisingly, the degree of modification made little difference to the uptake of H_2, as the increase in uptake with a greater number of phenyl groups is counter-balanced by the increased mass of the material after modification.

Post-synthetic modification of bdc-NH_2 is not restricted to IRMOF-3. Gamez and co-workers showed that $[Gd_2(bdc\text{-}NH_2)_3(DMF)_4]$ **40** reacted with acetic acid to give $[Gd_2(bdc\text{-}NH_2)_{2.75}\{bdc\text{-}NHC(O)Me\}_{0.25}(DMF)_4]$ **41**.[37] They also demonstrated that the amine groups undergo reaction with isocyanates. Compound **40** reacted with EtNCO to give the urethane-modified MOF $[Gd_2(bdc\text{-}NH_2)_{2.8}(bdc\text{-}NHCO_2H)_{0.2}(DMF)_4]$ **42** following hydrolysis of the initially-formed urea, which was not observed. Only one of the three independent amino groups in **40** is capable of modification due to steric constraints.

Cohen and co-workers showed that **10** reacts with isocyanates too, although in this case urea-functionalised MOFs could be isolated.[38] They demonstrated that straight-chain alkyl isocyanates show decreasing conversion with increasing chain length, in a similar manner to the reactions with anhydrides. Thus, for example, 71% conversion was observed for the reaction with EtNCO, whereas 51% conversion was seen for $Me(CH_2)_4NCO$. Bulkier isocyanates showed even lower conversions, with only 27% for cyclohexyl isocyanate.

Tandem reactions with anhydrides and isocyanates have also been undertaken.[39] For example, reaction of **10** with decanoic anhydride followed by propyl isocyanate gave a MOF containing ~21% of each functionality, *i.e.* $[Zn_4O(bdc\text{-}NH_2)_{1.74}\{bdc\text{-}NHC(O)(CH_2)_8Me\}_{0.63}\{bdc\text{-}NHC(O)NHPr\}_{0.63}]$ **43**, which has three different functional groups (amine, amide and urea) in the pores. Further treatment of this material with allyl isocyanate followed by crotonic anhydride gave a material of the approximate composition $[Zn_4O(bdc\text{-}NH_2)_{0.6}\{bdc\text{-}NHC(O)(CH_2)_8Me\}_{0.72}\{bdc\text{-}NHC(O)NHPr\}_{0.54}\{bdc\text{-}$

NHC(O)NHCH$_2$CH=CH$_2$}$_{0.63}${bdc-NHC(O)CH=CHMe}$_{0.51}$] **44** (Scheme 2). This MOF has five different groups in the pores, illustrating the potential of post-synthetic modification in the preparation of MC-MOFs.

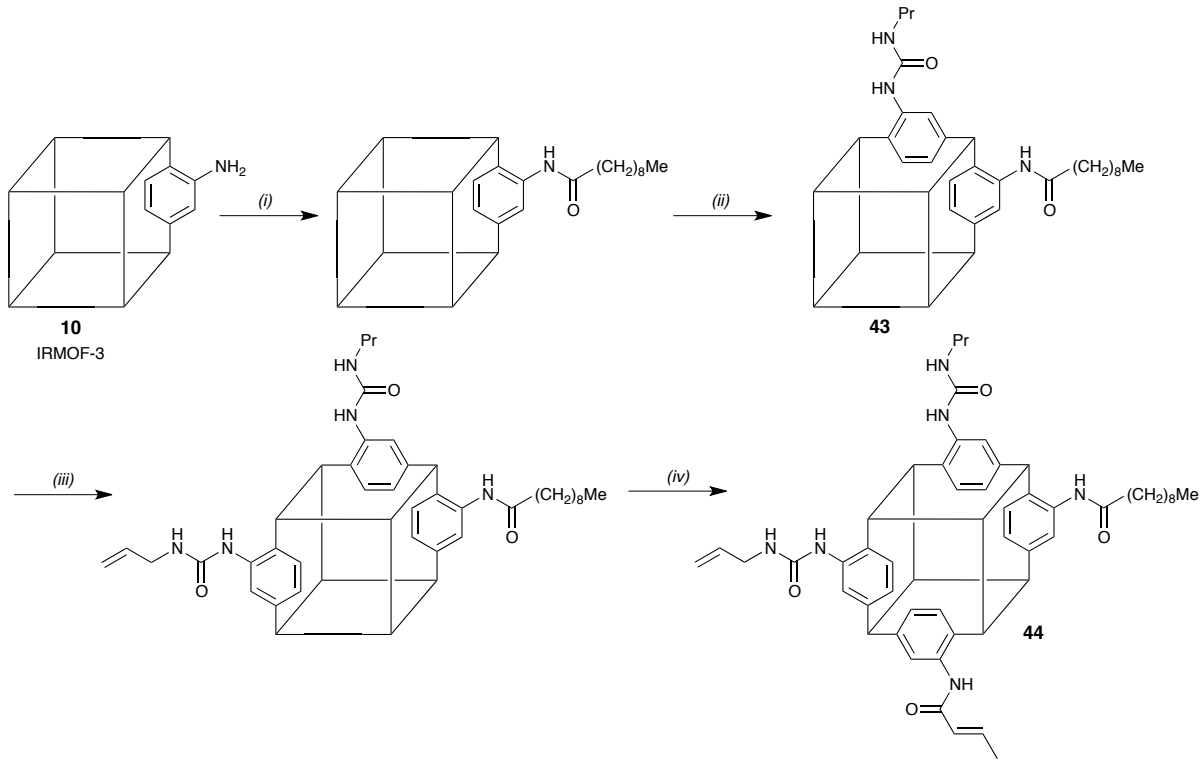

Scheme 2. (*i*) O{C(O)(CH$_2$)$_8$Me}$_2$, CHCl$_3$; *(ii)* PrNCO, CHCl$_3$; *(iii)* CH$_2$=CHCH$_2$NCO, CHCl$_3$; *(iv)* O{C(O)CH=CHMe}$_2$, CHCl$_3$.

Yaghi and co-workers investigated ring-opening reactions on **10**, as shown in Scheme 3. Elemental analyses suggested that the reaction with 1,3-propanesultone gave [Zn$_4$O(bdc-NH$_2$)$_{1.29}$(bdc-NHCH$_2$CH$_2$CH$_2$SO$_3$H)$_{1.71}$] **45**, whereas the reaction with 2-methylaziridine gave an average of 1.08 aziridine additions per linker, in turn suggesting a mixture of linkers in the product with zero, one and more additions.[40]

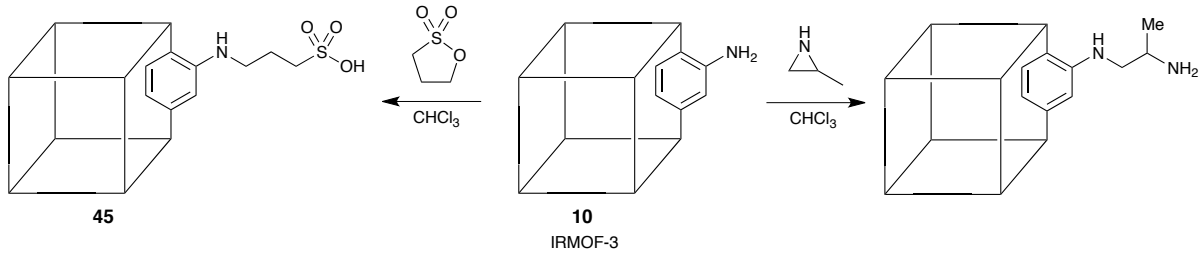

Scheme 3.

Rosseinsky and co-workers showed that the amine groups in **10** react with salicylaldehyde to convert the MOF into [Zn$_4$O(bdc-NH$_2$)$_{2.6}$(bdc-N=CHC$_6$H$_4$OH-2)$_{0.4}$] **46**.[41] The reaction of **46** with [VO(acac)$_2$] led to complete metallation of the salicylidene (Scheme 4). The vanadium-containing MOF **47** was shown to catalyse the oxidation of cyclohexene with ^{t}BuOOH.

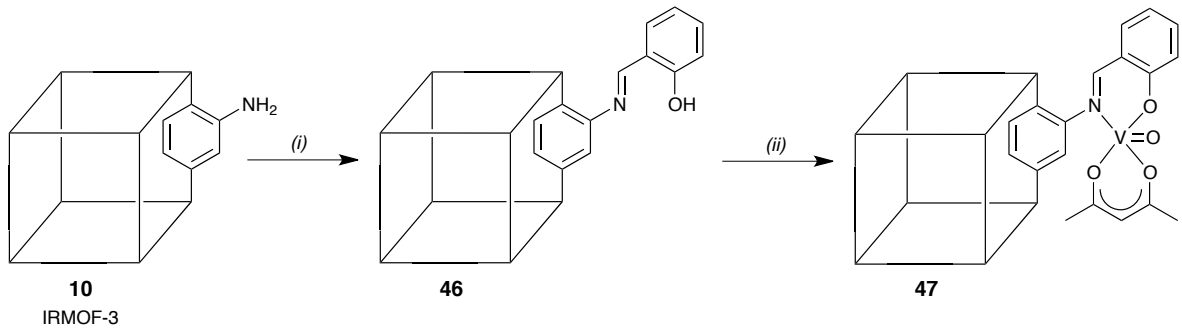

Scheme 4. *(i)* salicylaldehyde, toluene; *(ii)* $VO(acac)_2$, CH_2Cl_2.

In a related study, Corma and co-workers reported a similar reaction of **10** with salicylaldehyde, though under their conditions only 3 % conversion could be achieved without framework collapse.[42] The mixed-ligand MOF was then treated with $[AuCl_4]^-$, leading to metallation of all of the salicylidene groups. The gold-containing product was used as a catalyst for coupling and cyclisation reactions.

Reactions on zinc MOFs are not limited to IRMOF-3 (**10**), and the Cohen group have investigated analogous reactions with $[Zn_4O(bdc\text{-}NH_2)(btb)_{4/3}]$ **48** (UMCM-1-NH_2) and $[Zn_2(bdc\text{-}NH_2)_2(dabco)]$ **49** (DMOF-1-NH_2).[43] The reactions of **49** with linear anhydrides led to lower conversions than analogous reactions of **10** under similar conditions, whereas those of the larger pore MOF **48** led to higher conversions. Thus, for example, the reaction with excess decanoic anhydride at 55 °C for 24 h gave 34 % conversion for **49**, 46 % conversion for **10** and 89 % conversion for **48**.

Modification of **48** with 3-hydroxylphthalic anhydride and 2,3-pyrazinedicarboxylic anhydride gave the MOFs $[Zn_4O(bdc\text{-}NH_2)_{0.65}(H\mathbf{L^1})_{0.35}(btb)_{4/3}]$ **50** and $[Zn_4O(bdc\text{-}NH_2)_{0.5}(H\mathbf{L^2})_{0.5}(btb)_{4/3}]$ **51** respectively.[44] These products both contain uncoordinated donor groups, which can bind to iron, copper or indium centres. Iron derivatives of **50** were shown to catalyse the Mukaiyama-aldol reaction, whereas indium derivatives catalyse epoxide ring-opening reactions.[45]

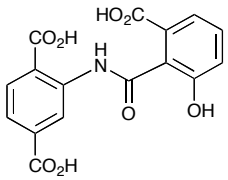

$H_3\mathbf{L^1}$

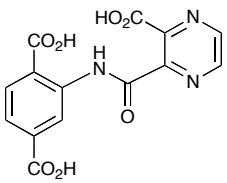

$H_3\mathbf{L^2}$

The 2-amino-1,4-benzenedicarboxylate analogue of [Al(OH)(bdc)] (**24**, MIL-53(Al))[46] has been prepared, and shown to react with anhydrides in a similar manner to the zinc systems.[47] As expected, the conversion of $[Al(OH)(bdc\text{-}NH_2)]$ **52** to $[Al(OH)(bdc\text{-}NH_2)_{1-x}\{bdc\text{-}NHC(O)(CH_2)_nMe\}_x]$ **53** was dependent on the alkyl chain length. So, acetic anhydride (n = 0) gave **53a** with x = 0.91, whereas octanoic anhydride (n = 6) gave **53b** with x = 0.17. Increase in the alkyl chain length has been shown to increase the hydrophobicity of the material, with **53b** being superhydrophobic, having water contact angles greater than 150°.[47]

Compound **52** was reacted with diphosgene or thiophosgene in THF to form the cyanate-functionalised MOF $[Al(OH)(bdc\text{-}NH_2)_{0.1}(bdc\text{-}NCO)_{0.9}]$ **54** and the thiocyanate functionalised MOF $[Al(OH)(bdc\text{-}NH_2)_{0.1}(bdc\text{-}NCS)_{0.9}]$ **55** respectively.[48] These MOFs were further reacted with alcohols to form carbamates or thiocarbamates, and with amines to form

ureas or thioureas, with the extent of the reactions depending on the size of reagent. These transformations are summarised in Scheme 5.

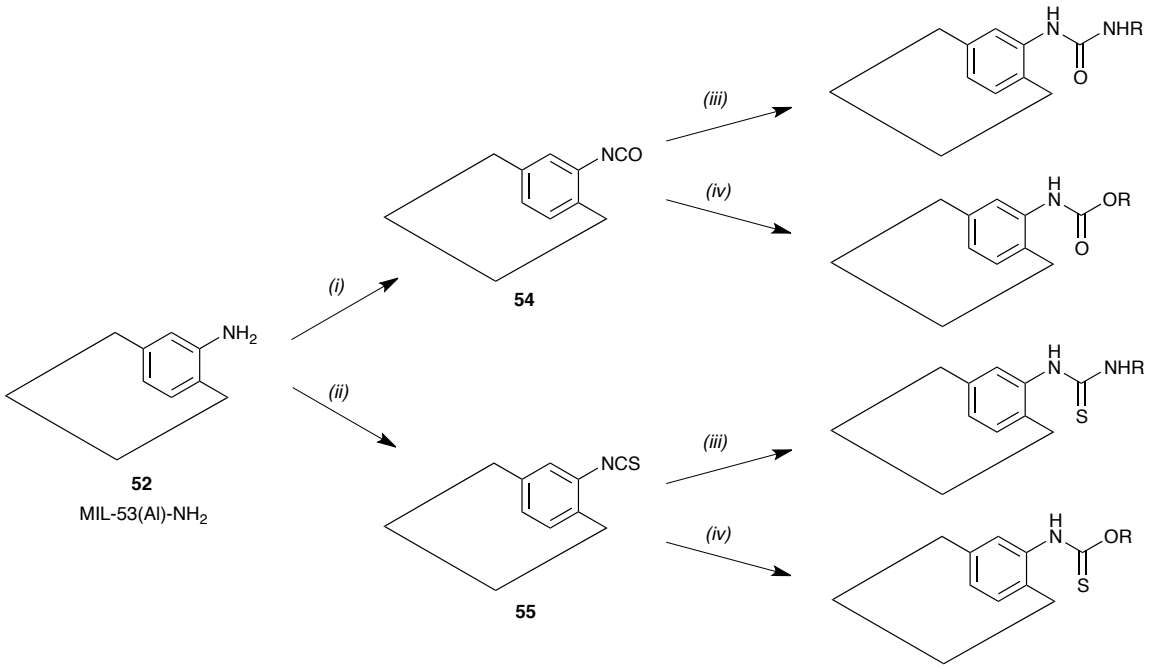

Scheme 5. *(i)* $C(O)Cl_2$; *(ii)* $C(S)Cl_2$, 55 °C; *(iii)* RNH_2 (R = Pr, Bu, Ph, Cy), MeCN, 80 °C; *(iv)* ROH (R = Me, Et, Bu), 65-100 °C.

While the majority of post-synthetic modification reactions have involved reactions of pendant amine groups, there are a number that have employed different chemistry. Cohen reported the bromination of an alkene as part of a tandem reaction (see above).[35] This process was studied in more detail by Bauer and co-workers.[49] They reported the stilbene-based MOF $[Zn_4O(sdc)_3]$ **56** (sdc = *trans*-4,4'-stilbenedicarboxylate), and showed that bromination with Br_2 in chloroform gave 60% conversion after 48 h. Interestingly, only the *meso* isomer of 4,4′-(1,2-dibromoethane-1,2-diyl)dibenzoate was observed. Incorporation of the dicarboxylate as part of the MOF prevents C–C rotation and, as a consequence, no *rac* isomer was produced. This is in contrast to control reactions with solid Na_2sdc which gave a mixture of the *meso* and *rac* isomers of the brominated dicarboxylate.

Burrows and co-workers showed that the aldehyde-functionalised MOF $[Zn_4O(bpdc\text{-}CHO)_3(H_2O)_2]$ **57** reacts incompletely with 2,4-dinitrophenylhydrazine to give $[Zn_4O(bpdc\text{-}CHO)_{1.2}(bpdc\text{-}CH{=}NNHAr)_{1.8}(H_2O)_2]$ (Ar = 2,4-dinitrophenyl) **58** (Scheme 6).[19] The crystal structure of **58**, shown in Figure 9, revealed that the two doubly-interpenetrated networks move closer together on incorporation of the bulky hydrazone groups. To get around the issue of incomplete modification, the same process was carried out on $[Zn_4O(bpdc\text{-}CHO)_{0.3}(bpdc\text{-}OMe)_{2.7}]$ **9**. In this case, post-synthetic modification with 2,4-dinitrophenylhydrazine gave complete conversion of the aldehyde groups to hydrazone groups and formation of $[Zn_4O(bpdc\text{-}CH{=}NNHAr)_{0.3}(bpdc\text{-}OMe)_{2.7}]$ **59**.

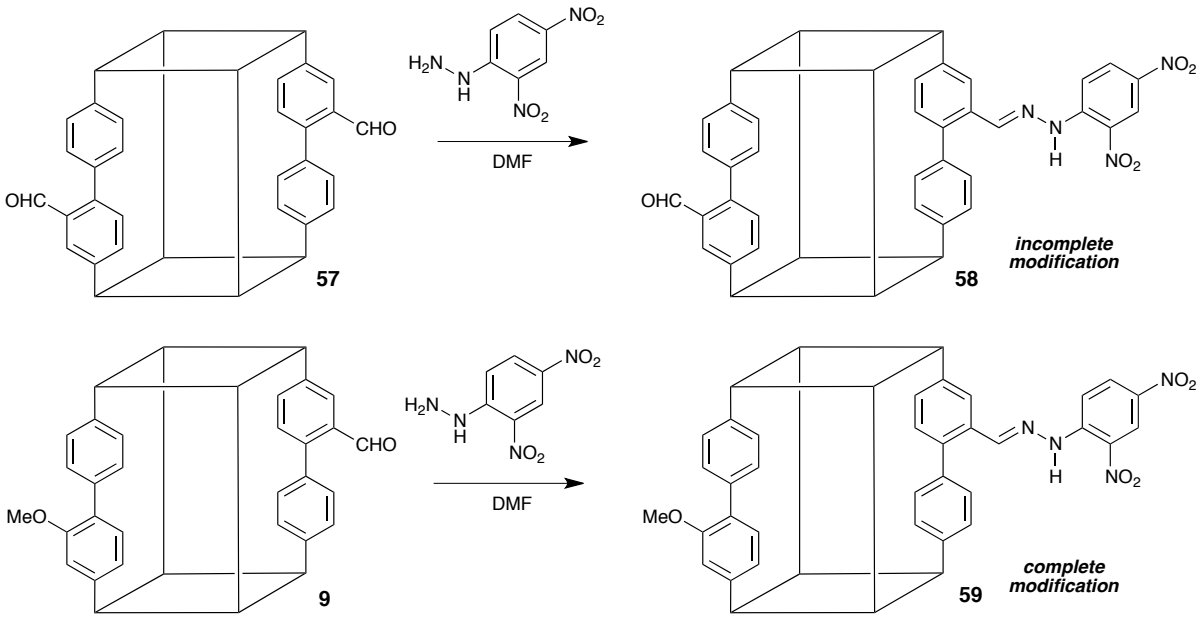

Scheme 6

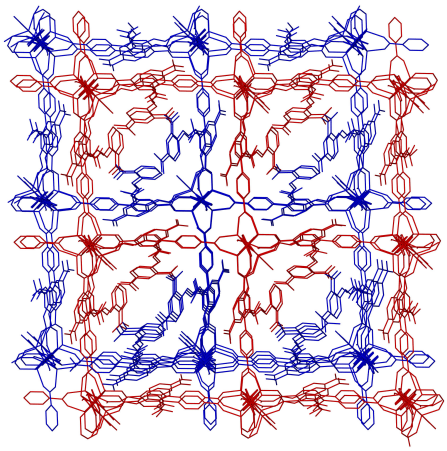

Figure 9. Part of the crystal structure of $[Zn_4O(bpdc\text{-}CHO)_{1.2}(bpdc\text{-}CH{=}NNHAr)_{1.8}(H_2O)_2]$ **58**, with the two interpenetrated networks shown in different colours.

Burrows and co-workers also reported the first example of a post-synthetic oxidation in MOF chemistry.[50] They showed that the sulfide-tagged MOF $[Zn_4O(bpdc\text{-}CH_2SMe)_3(DMF)_2]$ **60** reacted with dimethyldioxirane (DMDO) to give 23 % conversion to the sulfone-tagged MOF **61** (Scheme 7).

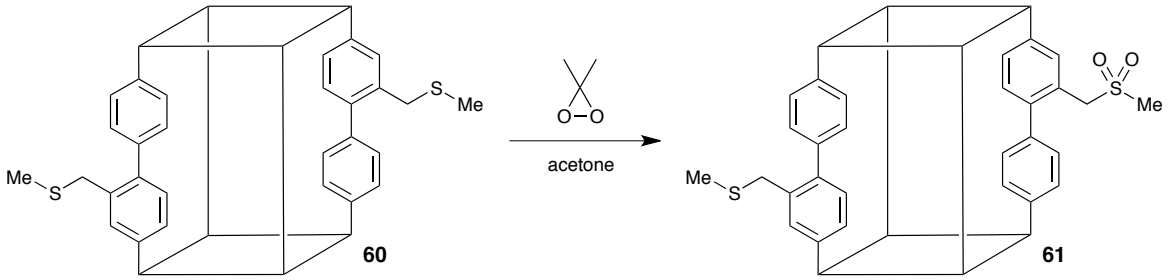

Scheme 7

Yaghi and co-workers reported a zinc network containing an aldehyde-functionalised imidazolate.[51] The compound [Zn(im-CHO)$_2$] **62** (ZIF-90) was reduced by sodium borohydride in methanol in the first example of a post-synthetic reduction on a network material. The reaction proceeded with approximately 80% conversion to give [Zn(im-CHO)$_{0.4}$(im-CH$_2$OH)$_{1.6}$] **63** (ZIF-91), as shown in Scheme 8.

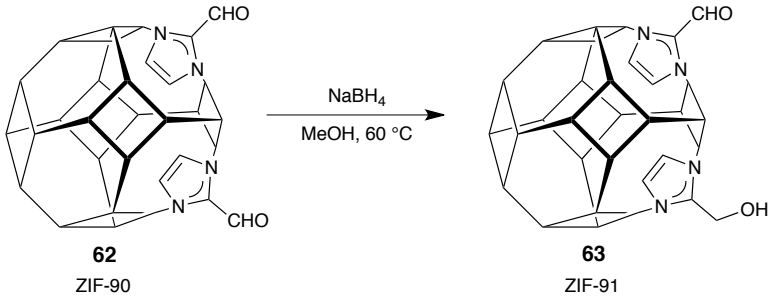

62 ZIF-90 **63** ZIF-91

Scheme 8

Kitagawa and co-workers recently demonstrated that photochemical activation of [Zn$_2$(1,3-bdc-N$_3$)$_2$(4,4'-bipy)] **64** (1,3-bdc-N$_3$ = 5-azido-1,3-benzenedicarboxylate) occurred in a single-crystal-to-single-crystal transformation, converting some of the azide groups into nitrenes, and giving a product that was crystallographically characterised as [Zn$_2$(1,3-bdc-N$_3$)$_{1.36}$(1,3-bdc-N)$_{0.64}$(4,4'-bipy)] **65**. The photogenerated nitrene reacts with O$_2$ to form a mixture of nitro (-NO$_2$) and nitroso- (-NO) groups.[52]

Lin and co-workers undertook post-synthetic modification reactions on [Fe$_3$O(Cl)(H$_2$O)$_2$(bdc)$_{2.48}$(bdc-NH$_2$)$_{0.52}$] **66**. They showed that **66** could be modified with imaging contrast agents and *cis*-platin pro-drugs to give materials such as [Fe$_3$O(Cl)(H$_2$O)$_2$(bdc)$_{2.48}$(bdc-NH$_2$)$_{0.31}$(L)$_{0.21}$] (**67**, L = **L^3**; **68**, L = **L^4**).[22]

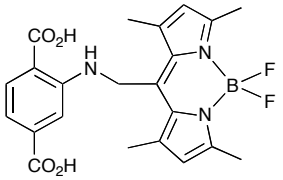

H_2**L^3**

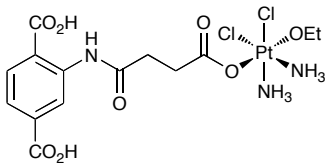

H_2**L^4**

Post-synthetic coordination of available donor sites on a ligand to an added metal centre can also occur incompletely. Lin and co-workers showed that [Cd$_3$Cl$_6$(H$_2$**L^5**)$_3$] **69** (Figure 10) reacts with Ti(O^{i}Pr)$_4$ to form [Cd$_3$Cl$_6$(H$_2$**L^5**)$_2${**L^5**Ti(O^{i}Pr)$_2$}] **70**.[53] In this case, two of the H$_2$**L^5** ligands remain unfunctionalised as they interact strongly with each other through hydrogen bonding and π···π interactions. As a consequence, these groups are unavailable for reaction with titanium. Compound **70** has been used as a chiral catalyst for diethylzinc additions to aromatic aldehydes.

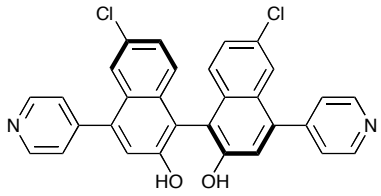

H_2**L^5**

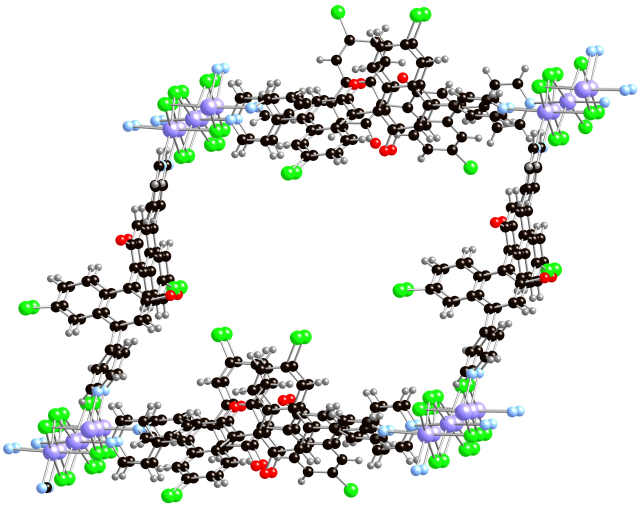

Figure 10. Part of the structure of $[Cd_3Cl_6(H_2\mathbf{L}^5)_3]$ **69**, with cadmium atoms purple, oxygen atoms red, nitrogen atoms blue, chlorine atoms green, carbon atoms black and hydrogen atoms grey.

As the chemistry described in this section illustrates, post-synthetic modification is a good method for producing MC-MOFs, though the interplay of the different functional groups present in the pores is only just starting to be studied.[54]

2.5 MC-MOFs formed via post-synthetic modification of the metal coordination sphere

Post-synthetic modification of MOFs is not restricted to organic transformations on the bridging ligands, and can also involve changes in the metal coordination environment. If these reactions do not go to completion, MC-MOFs will result. Kim and co-workers studied the substitution of the labile aqua ligands in $[Cr_3O(H_2O)_2F(bdc)_3]$ (MIL-101) with the L-proline-functionalised pyridine ligands $\mathbf{L}^6$ and $\mathbf{L}^7$ to form the chiral MOFs $[Cr_3O(\mathbf{L}^6)_{1.8}(H_2O)_{0.2}F(bdc)_3]$ **71** and $[Cr_3O(\mathbf{L}^7)_{1.75}(H_2O)_{0.25}F(bdc)_3]$ **72** and used these as catalysts in asymmetric aldol reactions.[55] They demonstrated that **71** and **72** show higher enantioselectivity than the use of $\mathbf{L}^6$ or $\mathbf{L}^7$ alone.

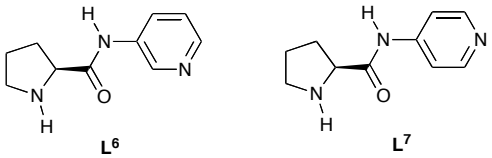

$\mathbf{L}^6$ $\mathbf{L}^7$

Rosseinsky and co-workers substituted the labile water ligands in $[Cu_3(btc)_2(H_2O)_3]$ **73** (HKUST-1) for 4-(methylamino)pyridine (map) ligands giving $[Cu_3(btc)_2(map)_x(H_2O)_{3-x}]$ **74** ($0.96 \leq x \leq 2.91$).[56] They showed that the 60 %-functionalised material $[Cu_3(btc)_2(map)_{1.8}(H_2O)_{1.2}]$ **74a** adsorbs NO, converting the secondary amine into an *N*-diazenium diolate. The reaction mechanism requires two neighbouring map ligands, so that the intermediate protonated *N*-diazenium diolate can offload a proton, which converts the neighbouring map ligand into an ammonium ion (Scheme 9). These ions have been detected spectroscopically. When the loading of map is 32 %, no *N*-diazenium diolate formation was observed, presumably due to the small number of pores with neighbouring map ligands. In contrast, if the loading of map is 97 %, NO adsorption was not observed, presumably due to

blockage of the pores. This is therefore a good example of a MC-MOF in which the proportion of the different ligands is vital to the function.

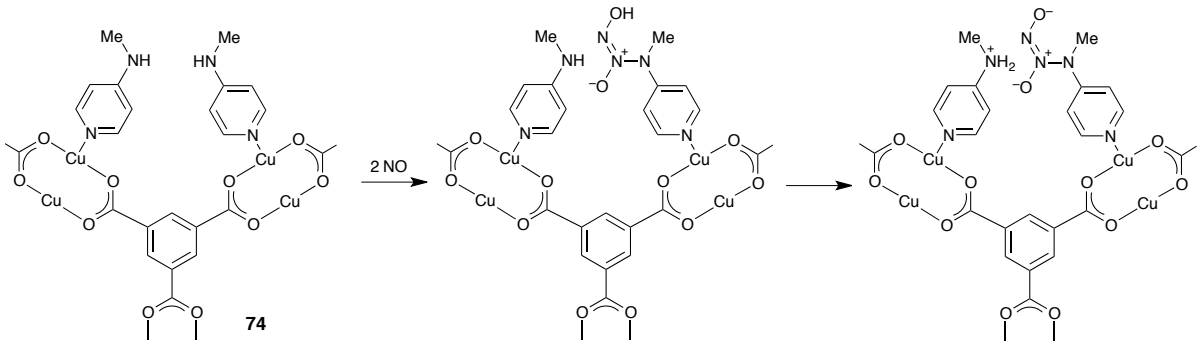

Scheme 9

Recently, Cohen and co-workers showed that the amino groups in **10** and **48** also react with NO to form *N*-diazenium diolates, with thermogravimetric analyses suggesting greater conversion for **48**.[57] Both the copper and zinc *N*-diazenium diolates slowly release NO gas, suggesting they have potential for medical applications.

2.6 Characterisation of mixed-ligand MOFs

Characterisation of mixed-ligand MC-MOFs can be problematic. Positional disorder of substituents on a particular ligand coupled with spatial disorder of the different ligands restricts the amount of information that can be obtained from crystallography, especially given the relatively weak diffraction that is often observed for porous MOF materials. Despite these limitations, some mixed-ligand MOFs have been crystallographically characterised. For example, Burrows and co-workers were able to model structures containing 2,4-dinitrophenylhydrazone and either a methoxy or a formyl group,[19] whereas Yaghi and co-workers have crystallographically characterised mixed-dicarboxylate MOFs containing up to four different linkers.[11]

NMR spectroscopy is the most routine method of characterisation for mixed-ligand MOFs. The MOFs are typically digested in acid or base, and the resultant solutions analysed by ^{1}H NMR spectroscopy.[33] The integrals observed provide a good indication of the relative degrees of incorporation of the different ligands. Zinc MOFs are relatively straightforward to digest in acid, but the MIL-53(Al) materials require more forcing conditions to dissolve.[48] Solid state NMR spectroscopy can be used to analyse MOFs without digestion. Yaghi and co-workers used ^{13}C CP/MAS NMR spectra to show the incorporation of different dicarboxylates into MC-MOFs.[11]

NMR studies on a bulk sample, however, cannot distinguish between a solid solution, in which two different ligands are mixed at a molecular level, and a mechanical mixture of crystals of two compounds. There are several methods by which these two possibilities can be distinguished. The first involves carrying out analyses on individual single crystals. The Burrows and Cohen groups used ESI mass spectra of digested individual single crystals to show that each crystal contained the two different ligands.[19, 34, 50] In order to rule out the possibility that crystals of MC-MOFs contain macroscopic domains of different functionalities, Yaghi and co-workers prepared large single crystals of MC-MOFs including

14 and **15** that were then dissected into three equal segments. These were each digested and analysed by ^{1}H NMR spectroscopy, which demonstrated identical link ratios in each segment.[11]

The Baiker[10, 20] and Kitagawa[21] groups have used high resolution powder X-ray diffraction to show single phases were present in MC-MOFs. The powder X-ray diffraction studies on MOFs in the series $[Zn_4O(bdc)_{3-x}(bdc\text{-}NH_2)_x]$ **12**, for example, show a linear shift in the peak positions with increasing proportion of bdc-NH_2 in the product, as shown in Figure 11. This follows Vegard's Law and is consistent with a random distribution of the two linkers. A mechanical mixture of $[Zn_4O(bdc)_3]$ (**11**, MOF-5) and $[Zn_4O(bdc\text{-}NH_2)_3]$ (**10**, IRMOF-3) would give separate peaks for each material, and this would appear as peak splitting, which was not observed.

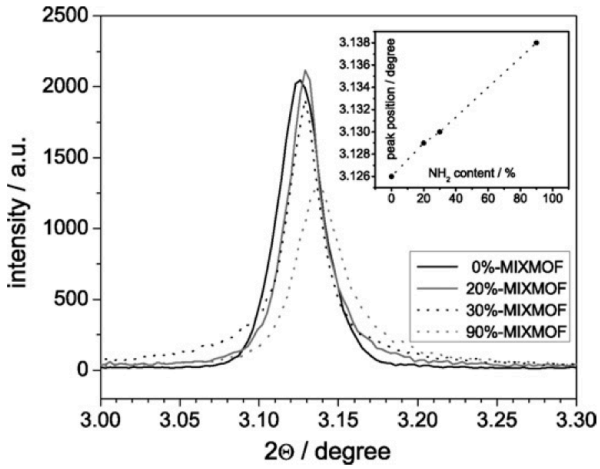

Figure 11. Peak shift of the $[Zn_4O(bdc)_{3-x}(bdc\text{-}NH_2)_x]$ (**12**) series observed using high-resolution powder X-ray diffraction. *x* %-MIXMOF refers to the percentage of bdc-NH_2 present in the sample. Reprinted with permission from ref. [20].

Baiker and co-workers have also used thermogravimetric analysis to support the presence of MC-MOFs in the $[Zn_4O(bdc)_{3-x}(bdc\text{-}NH_2)_x]$ (**12**) series.[10, 20] The results showed that increasing the proportion of bdc-NH_2 led to a decrease in the thermal stability of the MOF. Under oxidising conditions, MOF-5 was observed to be stable to 450 °C, whereas $[Zn_4O(bdc)_{2.7}(bdc\text{-}NH_2)_{0.3}]$ began to decompose at 400 °C. The differences were most clearly seen in DTG plots (first differentials of the thermogravimetric analyses), where the observation of a single maximum for each compound is consistent with the presence of single phase materials.

3. Mixed-metal MOFs

In addition to inclusion of more than one linker, it is possible to form MC-MOFs by using more than one type of metal centre in the synthesis. This is shown schematically in Figure 12.

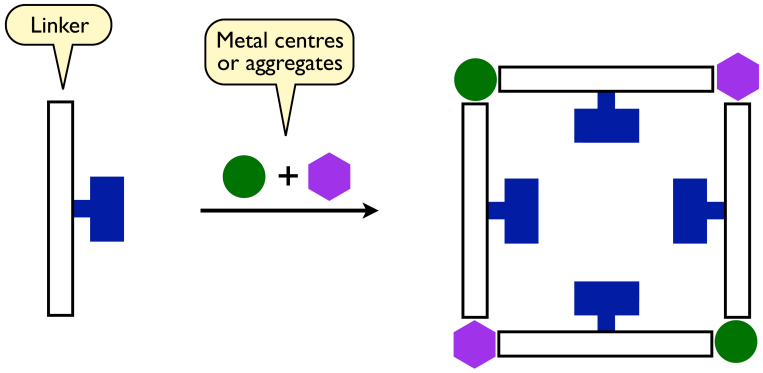

Figure 12. Schematic representation of the formation of a mixed-metal MOF through use of different metal centres in the synthesis.

3.1 Mixed-metal MOFs with d-block metals

Vujovic and co-workers showed that the reaction between $Cd(NCS)_2$ and *n*-abn (*n* = 2, 3, 4; abn = aminobenzonitrile) gave $[Cd(NSC)_2(n\text{-abn})_2]$, the structures of which consist of one-dimensional chain polymers with the metal centres bridged by pairs of NCS^- ligands.[58] For 3-abn, the product is isostructural with that of the nickel analogue. Addition of $Ni(NCS)_2$ to the reaction mixture gave $[Cd_{1-x}Ni_x(NSC)_2(3\text{-abn})_2]$ **75**, with $0.30 \geq x \geq 0.77$. Four crystal structures of mixed-metal MC-MOFs were obtained, one of which is shown in Figure 13. Electron microscopy confirmed the homogeneity of the mixed-metal compounds, and the Cd:Ni ratios obtained were in good agreement with those from the crystal structure determinations, with on average a slight excess of nickel over the proportion in the reaction mixture. The variation of unit cell parameters within the series follows Vegard's Law. DSC experiments revealed that the thermal stability of the products increases with an increasing proportion of nickel.

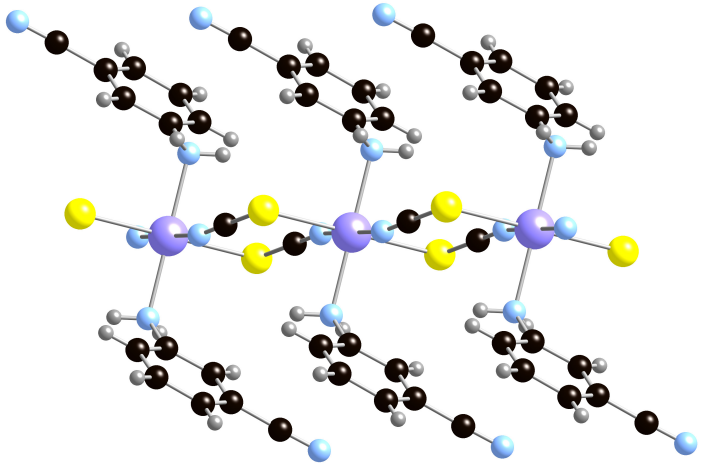

Figure 13. Part of the structure of $[Cd_{0.70}Ni_{0.30}(NSC)_2(3\text{-abn})_2]$ **75a**, with metal atoms purple, nitrogen atoms blue, sulfur atoms yellow, carbon atoms black and hydrogen atoms grey.

Chen, Gao and co-workers prepared several isostructural networks with the formula $[Co_xNi_{2-x}(ca)_2(dimb)]$ **76** ($0 \leq x \leq 2$, ca = D-(+)-camphorate, dimb = 1,4-di-(1-

imidazolylmethyl)benzene).[59] The structures consist of (4,4)-layers containing $[M_2(O_2CR)_4]$ secondary building units linked by the chiral camphorate ligands, shown in Figure 14, that are pillared by dimb ligands into a three-dimensional framework. The magnetic properties are consistent with the presence of random mixed-metal pairs. The Co:Ni ratios in the products were determined by a combination of ICP spectroscopy and X-ray photoelectron spectroscopy on the crystal surfaces and are broadly similar to those in the reaction mixtures.

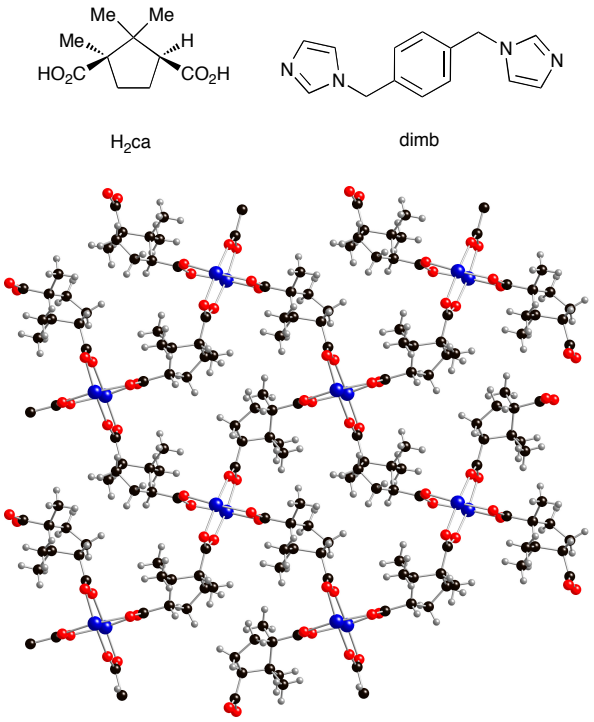

Figure 14. Part of the two-dimensional $M_2(ca)_2$ layers present in the structure of $[Co_{0.5}Ni_{1.5}(ca)_2(dimb)]$ **76a**. These are linked by pillaring dimb ligands into a three-dimensional network. Metal atoms are blue, oxygen atoms red, carbon atoms black and hydrogen atoms grey.

Schubert and co-workers found that the acid-catalysed reaction of a mixture of ZnO and CuO with imidazole led to mixed copper-zinc compounds of the general formula $[Zn_{1-x}Cu_x(im)_2]$ **77**. With the copper content less than 30 % (*i.e.* $x < 0.3$) **77** is isomorphous to a $[Zn(im)_2]$ phase, though with a higher proportion of copper new unidentified phases were observed. They were also able to dope small quantities of Mn^{2+}, Ni^{2+}, Co^{2+} and Ru^{2+} into $[Zn(im)_2]$.[60]

A theoretical study on substitutional doping of metal centres into MOF-5 (**11**) was reported in 2005. Fuentes-Cabrera and co-workers showed using DFT calculations that replacing one zinc atom per SBU with aluminium could alter the metallic properties of the MOF.[61] Botas and co-workers recently showed that cobalt(II) ions can be doped into MOF-5.[62] At low Co:Zn ratios, the uptake of cobalt was approximately equal to that in the reaction mixture, but at higher ratios the amount of included cobalt was reduced. These results suggest that a maximum of 25% of the zinc in MOF-5 (*i.e.* one atom per $Zn_4O(O_2CR)_6$ SBU) can be substituted by cobalt. The as-synthesised materials are pink, implying octahedral coordination of the cobalt, with it binding to two solvent (DEF) molecules. The cobalt-containing MOFs were activated by heating at 100 °C under vacuum. This caused a colour change to blue, which is consistent with loss of the coordinated solvent molecules from the

cobalt centres and conversion to tetrahedral geometry. The Co-doped MOFs show a slightly higher degree of H_2 adsorption than MOF-5.

Bu and co-workers reported a range of tetrazolate-based coordination polymers in which both cobalt and zinc are present.[63] In the compounds $[Co_{0.03}Zn_{0.97}(pt)_2]$ **78**, $[Co_{0.04}Zn_{0.96}(3\text{-tb})]$ **79** and $[Co_{0.04}Zn_{0.96}(4\text{-tb})]$ **80**, the presence of both metals was required to get crystalline products. The percentage of cobalt included in the products, estimated by ICP spectroscopy, was independent of that present in the reaction mixture, consistent with preferential inclusion of zinc. In contrast, the compound $[CoZn(2\text{-tb})_2(H_2O)_2]$ **81** contains a 1:1 ratio of Co and Zn, with the two metal centres independent in the asymmetric unit, and taking different structural roles.

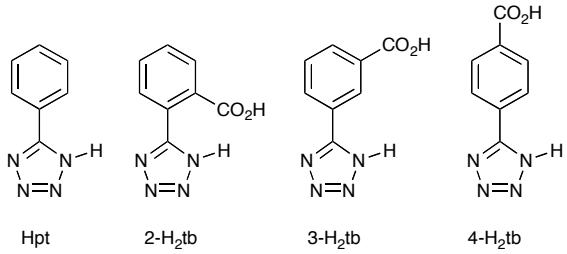

3.2 Mixed-metal MOFs with f-block metals

The first MOF to contain mixed lanthanides was reported in 1998. Perec and co-workers prepared $[LaM(oda)_3(H_2O)_3]$ **82** (oda = oxydiacetate; M = Gd, Y) and showed that these compounds form three-dimensional networks in which the two metal centres play different structural roles.[64]

Férey and co-workers reported the europium-doped yttrium 1,3,5-benzenetricarboxylate compound $[Y_{0.976}Eu_{0.024}(btc)]$ **83** (MIL-78(Y,Eu)). This was formed under hydrothermal conditions and shown by X-ray powder diffraction to have a three-dimensional structure (Figure 15).[65] Isostructural MOFs were formed with other lanthanide dopants, and efficient visible light emission was observed for the Eu-, Tb- and Dy-doped materials under UV irradiation, as shown in Figure 16.

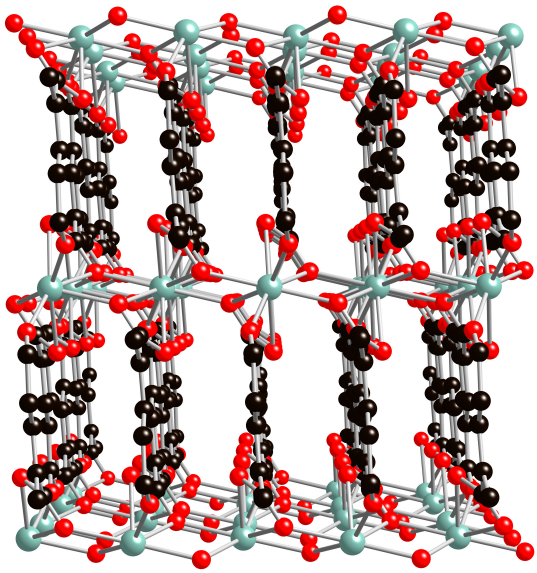

Figure 15. Part of the structure of $[Y_{0.976}Eu_{0.024}(btc)]$ **83**, with yttrium/europium atoms teal, oxygen atoms red and carbon atoms black. Hydrogen atoms have been omitted for clarity.

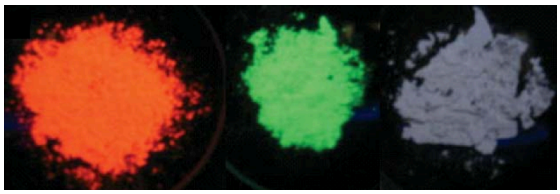

Figure 16. Photographs of $[Y_{0.976}Ln_{0.024}(btc)]$ under UV irradiation (excitation at 252 nm). From left to right, Ln = Eu (**83**, red), Tb (green) and Dy (blue).[65] Reproduced by permission of the Royal Society of Chemistry.

Several studies have looked at mixed terbium-europium networks, and demonstrated that on excitation, energy transfer from Tb^{3+} to Eu^{3+} occurs, which enhances the Eu^{3+} emissions. These observations provide good evidence that the Tb^{3+} and Eu^{3+} ions are in close proximity within the structure and not clustered within separate domains. Tan and co-workers prepared the 1D coordination polymer $[Eu_2(\mathbf{L^8})_3(NO_3)_6]$ **84** ($\mathbf{L^8}$ = 1,4-bis{[2'-benzylamineformyl)phenoxy]methyl}benzene) and showed that by doping Tb^{3+} into the reaction mixture the colour of the luminescence under UV irradiation was altered.[66]

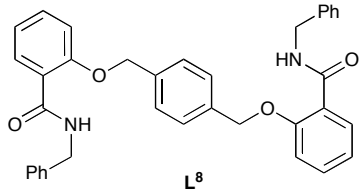

$\mathbf{L^8}$

Junk, Kynast and co-workers reported a series of compounds of the general formula $M[Ln(pic)_4]$ **85** (M = Na, NH_4; pic = 2-pyridinecarboxylate), in which pic-linked $[Ln(pic)_4]$ units form one-dimensional chains.[67] The compounds luminesce under UV excitation, and in mixed Tb/Eu compounds energy transfer from Tb^{3+} to Eu^{3+} occurred. The lanthanum analogues form different structures and energy transfer between the ligands was observed. Eu^{3+} and Tb^{3+}-doped samples of $[La(OH)(1,3\text{-bdc-}NH_2)]$ **86** (1,3-bdc-NH_2 = 5-amino-1,3-benzenedicarboxylate) also showed luminescent behaviour with characteristic emissions from the doped metal centres.[68]

Cahill and co-workers formed the mixed-lanthanide MOF $[EuTb(adipate)_3(H_2O)_2]\cdot$4,4'-bipy **87** *via* a hydrothermal reaction, and demonstrated that it has a 3D network structure, as shown in Figure 17.[69] Measurements of the luminescence behavior demonstrated that both the 4,4'-bipy guest molecules and the Tb^{3+} ions sensitise the Eu^{3+} ions, leading to a two-fold increase in the Eu^{3+} emission.

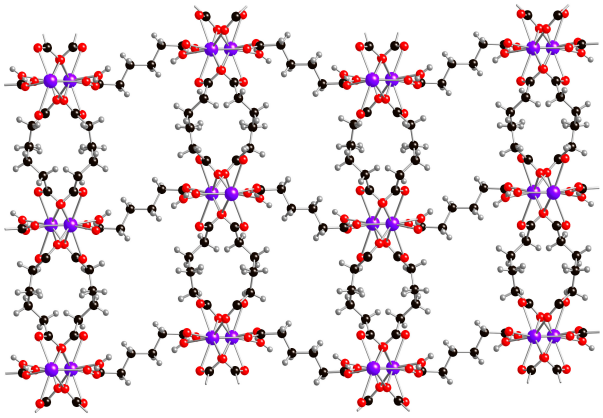

Figure 17. Part of the structure of $[EuTb(adipate)_3(H_2O)_2]\cdot$4,4'-bipy **87**, with lanthanide atoms purple, oxygen atoms red, carbon atoms black and hydrogen atoms grey. The included 4,4'-bipy molecules have been omitted for clarity.

Carlos, Nogueira and co-workers reported compounds of the general formula $[Ln_2(pdc)_2(pda)(H_2O)_2]$ (pdc = 2,5-pyridinedicarboxylate; pda = 1,4-phenylenediacetate), including the mixed-lanthanide MOFs $[Eu_{0.4}Tb_{1.6}(pdc)_2(pda)(H_2O)_2]$ **88a** and $[Eu_{0.2}Tb_{1.8}(pdc)_2(pda)(H_2O)_2]$ **88b**.[70] Photoluminescence studies on **88a,b** revealed the presence of effective Tb^{3+} to Eu^{3+} energy transfer at room temperature.

Thirumurugan and Cheetham introduced Tb^{3+} and Eu^{3+} ions into the bismuth MOFs $(NMe_2H_2)_2[Bi_4(bdc)_7(Him)]$ **89** and $(NMe_2H_2)[Bi(bdc)_2]$ **90**, showing that up to 20 % substitution was possible.[71] Intense ligand-sensitised luminescence was observed for the 2 %-doped materials.

Samples of $[La(btc)(H_2O)_6]$ **91** doped with either 5% Tb^{3+} or 1% Eu^{3+} were prepared by You and co-workers, and the presence of the dopant was shown not to affect the gross structure. The terbium- and europium-containing MOFs exhibited green and red emissions under UV light excitation, respectively.[72] The group also prepared the terbium analogue, $[Tb(btc)(H_2O)]\cdot 3H_2O$ **92**, and showed it has a structure in which helical strands are linked into a 3D framework.[73] On doping increasing amounts of Eu^{3+} ions into the framework, the luminescence of Tb^{3+} decreased and that of Eu^{3+} increased, and the emission spectra were consistent with efficient energy transfer from the Tb^{3+} to the Eu^{3+} ions. The photoluminescence colour changed from green to yellow, orange and red-orange on changing the proportion of the Eu^{3+} ions.

Petoud, Rosi and co-workers investigated the formation of mixed-lanthanide MOFs and studied their NIR spectra.[74] They demonstrated that Er^{3+} ions can be doped into the MOF $[Yb_2(pvdc)_3(H_2O)_2]$ **93** (pvdc = 4,4'-[(2,5-dimethoxy-1,4-phenylene)di-2,1-ethenediyl]bis-benzoate),[75] shown in Figure 18, at different ratios without changing the nature of the network. Energy-dispersive X-ray spectroscopy and ICP analyses were used to confirm that the ratio of lanthanides used in the synthesis were identical to those in the products. They also showed that there was a linear relationship between the relative intensities of the Yb^{3+} and Er^{3+} emissions in the NIR and their concentrations in the MOF. Incorporation of Nd^{3+} to give $[Nd_{0.18}Er_{1.10}Yb_{0.72}(pvdc)_3(H_2O)_2]$ **94** was also demonstrated, though the Nd^{3+} content was more difficult to control due to the larger difference in ionic radii and some size selectivity. The group postulated that these materials may be useful for bar-coding, as the

NIR emissions allow the unique proportions of lanthanides present in a particular material to be calculated. The NIR spectrum for **94** is shown in Figure 19.

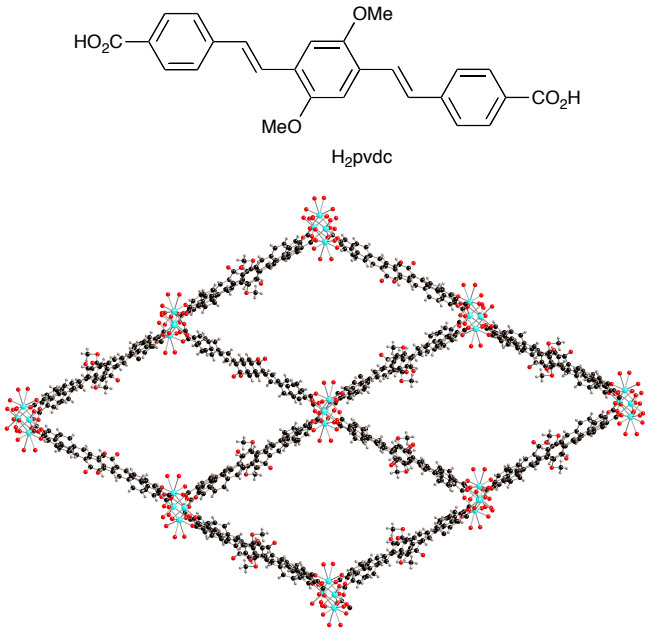

Figure 18. Part of the structure of $[Yb_2(pvdc)_3(H_2O)_2]$ **93**, with ytterbium atoms cyan, oxygen atoms red, carbon atoms black and hydrogen atoms grey.

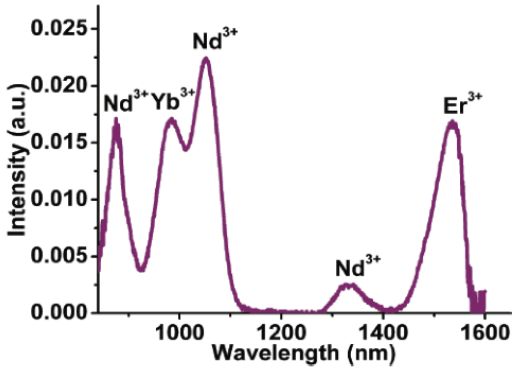

Figure 19. Yb^{3+}, Er^{3+} and Nd^{3+} emission from $[Nd_{0.18}Er_{1.10}Yb_{0.72}(pvdc)_3(H_2O)_2]$ **94** (λ_{ex} = 490 nm). Reprinted with permission from ref. [74].

3.3 Mixed-metal MOFs by post-synthetic modification

An alternative strategy for forming a mixed-metal MC-MOF is to substitute some of the metal centres in a pre-formed MOF by another metal in a post-synthetic modification reaction. This is shown schematically in Figure 20.

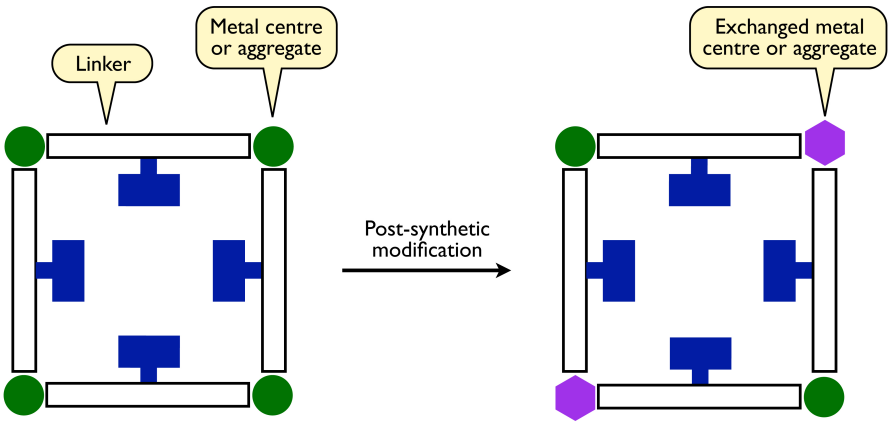

Figure 20. Schematic representation of the formation of a mixed-metal MOF through post-synthetic substitution of some of the metal centres in a MOF.

Kim and co-workers used this approach with $Cd_{1.5}(H_3O)_3[(Cd_4O)_3(\mathbf{L}^9)_8]$ **95**, and showed that this compound reversibly exchanges framework Cd^{2+} for Pb^{2+} without loss of crystallinity or structural integrity.[76] The substitution was 98 % complete after 2 hours and went to completion after 2 days in water, as witnessed by inductively coupled plasma atomic emission spectroscopy (ICP-AES), but mixed Cd-Pb MOFs were observed using shorter reaction times. The substitution is reversible, but the exchange of lead by cadmium is slower: the ICP-AES analysis showed approximately 50 % exchange of Pb^{2+} by Cd^{2+} in 1 day, with compete substitution taking 3 weeks.

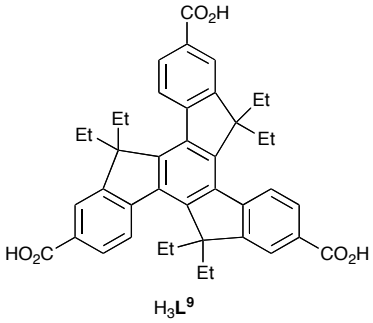

$H_3\mathbf{L}^9$

3.4 Mixed-valent state MOFs

MC-MOFs can also be formed with one metal centre, when it is present in two different oxidation states. There are several examples of this from iron chemistry.

Tarascon and co-workers prepared mixed-valent state MOFs by reducing $[Fe(OH)_{0.8}F_{0.2}(bdc)]$ **96** (MIL-53(Fe)) electrochemically in a cell with a lithium negative electrode.[77] The process is reversible and involves the uptake and removal of Li^+ ions together with the reversible reduction of Fe^{3+} into Fe^{2+}. Up to 0.6 Li^+ ions can be incorporated per formula unit without decomposition. Confirmation of the presence of both Fe^{2+} and Fe^{3+} was obtained from Mössbauer spectroscopy. Theoretical studies on this system showed that the reaction with lithium occurs through a two-step insertion/conversion mechanism.[78]

Mixed-valence state MOFs can also be prepared directly. Liu and co-workers prepared the iron-btc MOFs $[Fe_3(btc)_2(H_2O)_3]Cl_{1.5}$ **97**, which has the same framework as **73**, and

$[Fe_4Cl(btc)_{8/3}]Cl_2$ **98** from solvothermal reactions of iron(III) chloride, H_3btc and dabco.[79] The presence of both Fe^{2+} and Fe^{3+} in **97** and **98** was confirmed by Mössbauer spectroscopy. Kim and co-workers reported the mixed-valence MOF $[Fe_3O(bdc\text{-}F_4)_3(H_2O)_3]$ (bdc-F_4 = 2,3,5,6-tetrafluoro-1,4-benzenedicarboxylate) **99**.[80]

Chen, Long and co-workers prepared the mixed-valent MOF $[Fe_4O_2(chdc)_3]$ **100** (chdc = *trans*-1,4-cyclohexanedicarboxylate).[81] Mössbauer spectroscopy showed that below 155 K the Fe^{II} and Fe^{III} centres are localised, but above 225 K delocalisation occurs.

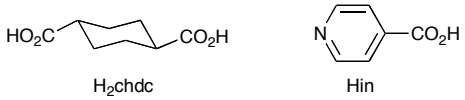

H_2chdc Hin

The formation of MC-MOFs with metals in two different oxidation states is not restricted to iron. Zamora and co-workers reported the mixed-valent copper MOF $[Cu_2Br(in)_2]$ **101** (in = 4-pyridylcarboxylate), which adopts a 2D layer structure.[82] Magnetic measurements revealed that the compound contains one unpaired electron per copper dimer, whereas electrical conductivity measurements confirmed the presence of weak electron delocalisation within each layer.

Fischer and co-workers recently showed that [VO(bdc)] **102** (MIL-47(V)) reacts with cobaltocene ($[Co(\eta^5\text{-}C_5H_5)_2]$) giving an inclusion compound in which the ratio of V:Co is 2:1. Spectroscopic and magnetic studies confirmed that the product is $[Co(\eta^5\text{-}C_5H_5)_2][VO(bdc)]_2$ **103**, with the included cobaltocene having been oxidised to cobaltocenium, and the framework containing a 1:1 mixture of V(III) and V(IV).[83]

4. Core shell MOFs

It has recently been demonstrated that in some circumstances, a MOF can grow epitaxially on the surface of a different MOF to give a heterogeneous material in which the shell and core of each crystal are not the same. The formation of core-shell MOFs has many features in common with the formation of solid solutions, since in both cases the lattice parameters of the two individual 'parent' crystal structures generally need to be closely related. As can be seen from the examples in Sections 2 and 3, this can be accomplished by variation of either the metal centres or the ligands. Two ways in which core-shell MOFs can be formed are shown schematically in Figure 21.

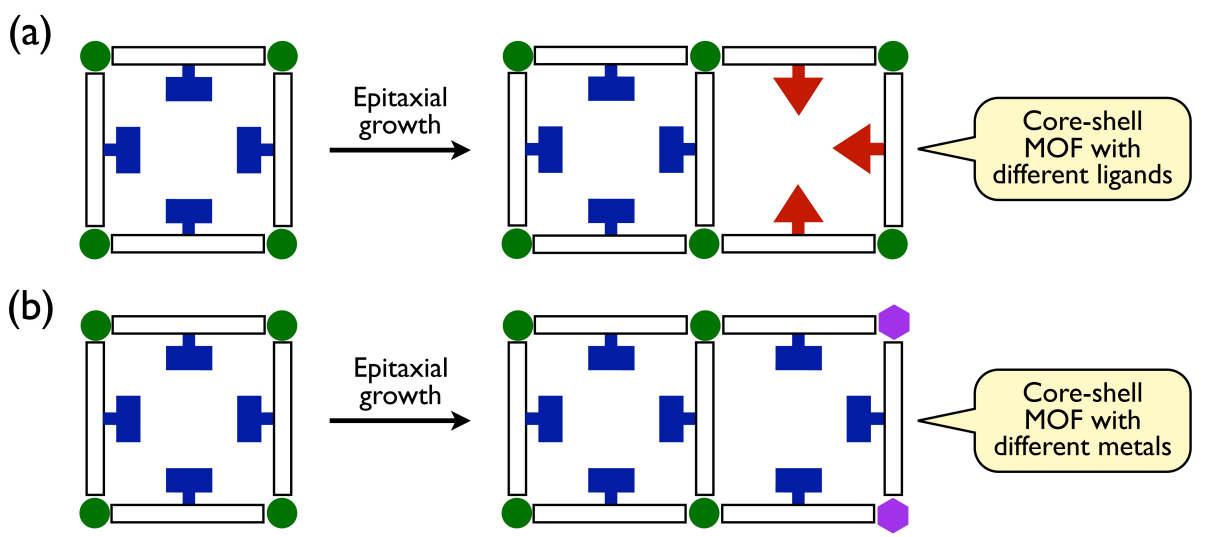

Figure 21. Schematic representation of the formation of the core-shell approach to forming MC-MOFs involving (a) different ligands and (b) different metals.

4.1 Core-shell MOFs formed using different metal centres

The first example of epitaxial growth of one MOF on the surface of another was reported by Kitagawa and co-workers, who focussed on the [M_2(dicarboxylate)$_2$(*N*,*N*′-donor ligand)] series of materials in their studies.[84] They took [Zn_2(1,4-ndc)$_2$(dabco)] **104** as the core crystal and [Cu_2(1,4-ndc)$_2$(dabco)] **105** as the shell crystal. Using an A@B nomenclature, where A denotes the shell MOF and B denotes the core MOF, they formed **105**@**104** by using crystals of **104** as seeds in a solution of copper(II) sulfate, 1,4-H_2ndc and dabco. Optical microscopy studies on single crystals showed colourless core crystals surrounded by a green shell. Prior to this, it had not been possible to obtain **105** as anything other than a powder.

Detailed X-ray analyses revealed a rotation of the shell crystal lattice of ~12° with respect to that of the core crystal on the (001) crystal surface, demonstrating that in-plane rotational epitaxial growth can compensate for the differences in lattice parameters in the core and shell crystals.

4.2 Core-shell MOFs formed using different ligands

In addition to the solid solutions of the general formula [$Zn_4O(bdc)_{3-x}(bdc\text{-}NH_2)_x$] **12** described in Section 2.1, Matzger and co-workers investigated the formation of core-shell MOFs using bdc and bdc-NH_2.[12] They took seeds of MOF-5 (**11**) and IRMOF-3 (**10**), grown over a period of 15 h in DEF, then placed each in the mother liquor of the other for a further 15 h. The resulting MOFs had core-shell structures, as clearly illustrated by their appearances. IRMOF-3@MOF-5 **106** is colourless in the centre and orange on the outside, whereas MOF-5@IRMOF-3 **107** is orange in the centre, and colourless on the outside. Crystals of **106** and **107** are shown in Figure 22. The group further demonstrated that a third layer could be added, giving materials such as MOF-5@IRMOF-3@MOF-5 **108**, and denoted these triple layer MOFs as Matryoshka MOFs from the similarity in appearance with Russian nested dolls.

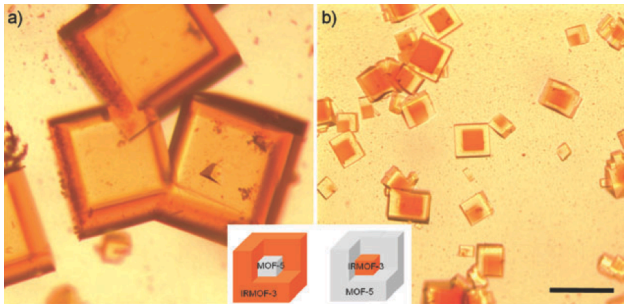

Figure 22. Microscope images of the core-shell MOFs (a) IRMOF-3@MOF-5 **106**, and (b) MOF-5@IRMOF-3 **107**. Scale bar, 200 mm.[12] Reprinted by permission of the Royal Society of Chemistry.

Jeong and Yoo have also reported core-shell MOFs based on MOF-5 and IRMOF-3.[85] They found it necessary to add an amine in the formation of IRMOF-3@MOF-5 **106** to prevent re-dissolution of the MOF-5 core crystals. X-ray diffraction studies revealed that the core-shell MOFs are connected at the single crystal level. Jeong and Yoo also showed that IRMOF-3/MOF-5 hybrid films could be grown on porous alumina supports. Under microwave conditions, MOF-5 readily nucleates on the supports, then IRMOF-3 can be grown onto these seed layers.

Kitagawa and co-workers used face-selective epitaxial growth to form BAB-type block MOF crystals.[86] Starting with [Zn_2(1,4-ndc)$_2$(dabco)] **104** as the core crystal, they grew [Zn_2(1,4-ndc)$_2$(dpn)] **109** on two opposite faces. Epitaxial growth of **109** only occurs at the (001) surfaces of **104** in the direction of the *c*-axis, which is the direction of the Zn–N coordination.

4.3 MC-MOFs formed through post-synthetic modification of crystal surfaces

Another type of core-shell MOFs are those in which post-synthetic modification has been used to chemically modify the external surfaces. In this case the shell is much thinner than when it has been grown onto a core crystal, but this approach is useful in changing the physical properties and reactivities of MOF crystals.

Hupp, Nguyen and co-workers explored this approach using the copper(I)-catalysed Huisgen cycloaddition reaction, also known as the 'click' reaction, which is used to couple a terminal alkyne and an azide into a triazole. They prepared [Zn_2(2,6-ndc)$_2$(**L**^{10})] **110** (**L**^{10} = 3-[(trimethylsilyl)ethynyl]-4-[2-(4-pyridinyl)ethenyl]pyridine), which contains a silyl-protected terminal alkyne, then used NBu_4F (TBAF) to remove the trimethylsilyl groups on the alkynes (Scheme 10).[87] They reasoned that given the bulk of the tetrabutylammonium cations, this deprotection would only occur on the external surfaces of the MOF crystals. To verify this, they then reacted the MOF with ethidium bromide monoazide ([N_3-eth]Br) in a 'click' reaction. The resultant MOF was fluorescent only on the external surfaces, confirming that addition of the ethidium groups was restricted to these surfaces. Using UV-visible absorption spectra, they estimated that less than 0.8% of the dipyridyl ligands in the bulk material had undergone cycloaddition. They also demonstrated that the crystal surfaces could be made more hydrophilic by modification with polyethyleneglycol chains.

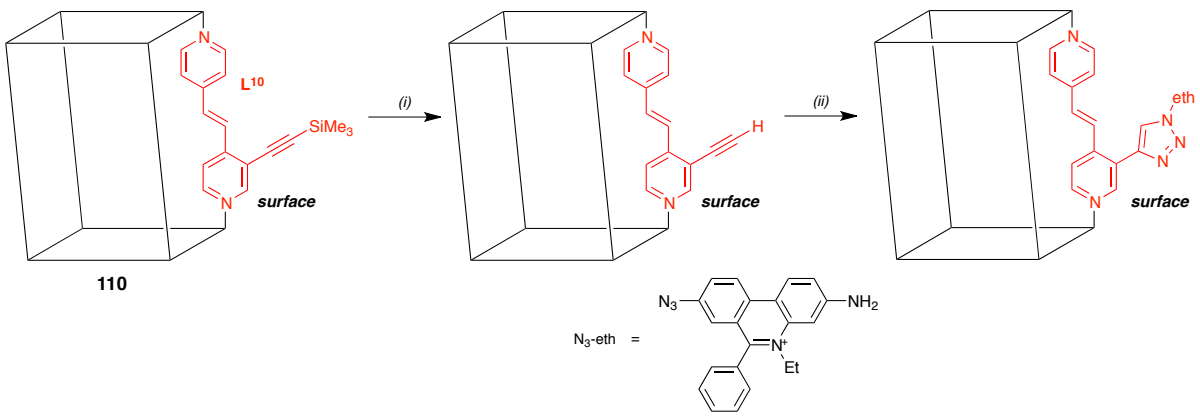

Scheme 10. *(i)* NBu_4F, THF; *(ii)* [N_3-eth]Br, $CuSO_4$, sodium ascorbate, DMF.

In an extension of these studies, they investigated similar chemistry with [Zn_2(tcpb)(**L**^{10})] **111** (tcpb = 1,2,4,5-tetrakis(4-carboxyphenyl)benzene), which in contrast to **110** is non-interpenetrated, thus containing larger pores (Figure 23).[88] Compound **111** was used to prepare MOFs in which both the surface and the interior of the crystals had been modified in different ways, as summarised in Scheme 11. Surface deprotection used aqueous potassium fluoride, and made use of the fact that, following solvent exchange, **111** is hydrophobic, thus preventing penetration of the KF into the pores. Subsequent reaction with ethidium bromide monoazide converted the terminal alkyne groups into triazoles, in a similar way to that observed with surface-deprotected **110**. The surface-modified **111** was treated with NEt_4F (TEAF) to deprotect the interior alkynes, followed by benzyl azide, which converted the interior terminal alkynes into triazoles. In this way, all of the silyl-protected alkyne groups were converted into triazoles, but with different substituents on the surfaces and in the interior of the crystals.

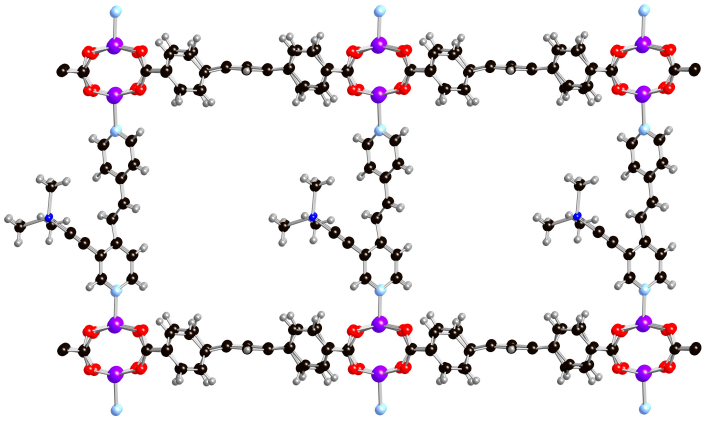

Figure 23. Part of the structure of [Zn_2(tcpb)(**L**^{10})] **111**, with zinc atoms purple, oxygen atoms red, nitrogen atoms pale blue, silicon atoms dark blue, carbon atoms black and hydrogen atoms grey.

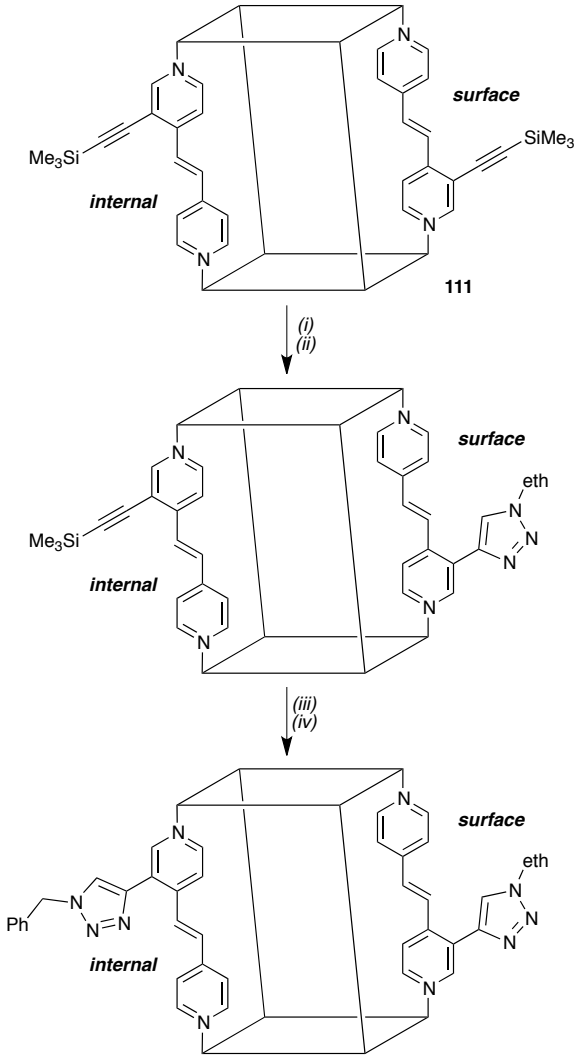

Scheme 11. *(i)* KF (aq); *(ii)* [N_3-eth]Br, $CuSO_4$, sodium ascorbate, DMF; *(iii)* NEt_4F, THF; *(iv)* $PhCH_2N_3$, $CuSO_4$, sodium ascorbate, DMF.

Kitagawa and co-workers have also investigated surface-modification reactions, though using coordination bond formation as opposed to covalent bond formation. They prepared the carboxylates $\mathbf{L}^{\mathbf{11\text{-}13}}$ which contain fluorescent dipyrromethene groups, and reacted these with **1** and **104**. The reaction only occurs at the crystal surfaces terminated by zinc-carboxylate bonds, and the bdc or 1,4-ndc ligands on these surfaces are substituted by $\mathbf{L}^{\mathbf{11\text{-}13}}$. The group employed confocal laser scanning microscopy to show that the modified MOFs fluoresce only at specific surfaces.[89]

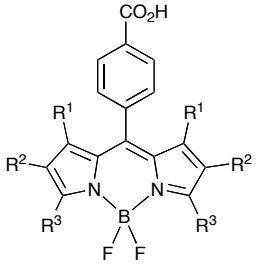

HL^{11}, R^1 = H, R^2 = H, R^3 = CH=CHPh
HL^{12}, R^1 = Me, R^2 = Et, R^3 = Me
HL^{13}, R^1 = Me, R^2 = H, R^3 = Me

Lin and co-workers have modified the external surfaces of nanoscale MOFs of the composition $[Ln(bdc)_{1.5}(H_2O)_2]$ (Ln = Eu, Gd, Tb) **112** with polyvinylpyrrolidone, and then

coated these nanoparticles with silica using a sol-gel method. Silica-coated nanoscale MOFs were further functionalised with a silylated Tb-EDTA monoamide derivative for the detection of DPA, which is a molecular marker in spore-producing bacteria such as anthrax.[90]

5. Conclusions

As the examples in Section 2 demonstrate, use of a mixture of ligands of similar structure, size and solubility in a MOF synthesis generally leads to the formation of a MC-MOF, with the ligands included in a disordered way into the same crystals, as opposed to a simple physical mixture of single-ligand MOFs. This is perhaps unsurprising given the entropic driving force towards mixing at the molecular level. In a similar manner, using a mixture of metal ions in the synthesis can also give rise to MC-MOFs, as shown by the examples in Section 3. This is most likely to occur if the metals are of similar size and have the same geometrical preferences, though the boundaries of when MC-MOFs do and do not form have yet to be probed.

In many cases, the two single-ligand or single-metal 'parent' MOFs are isostructural both with each other and the MC-MOFs, and when this is the case the lattice parameters of the MC-MOFs follow Vegard's Law. It is also possible, however, to include ligands or metals in MC-MOFs that do not form that structural type in the absence of a second linker or metal. For example, 2-nitro-1,4-benzenedicarboxylate (bdc-NO_2) does not form the compound $[Zn_4O(bdc\text{-}NO_2)_3]$, analogous to MOF-5, when it is used as the only linker, but it can be incorporated into the MOF-5 architecture in the MC-MOF $[Zn_4O(bdc)_{2.14}(bdc\text{-}NO_2)_{0.86}]$ **13**.[11] In a similar manner, cobalt nitrate does not react with H_2bdc to form the MOF-5 analogue $[Co_4O(bdc)_3]$, but up to 25% cobalt can be doped into the MOF-5 structure by using both zinc(II) and cobalt(II) nitrates in the synthesis.[62]

With MC-MOFs, there is often a direct correlation between the ratio of starting materials used in the synthesis and the ratio of the linkers or metal centres included in the product, as determined experimentally. This is not always the case, however, and sometimes preferential uptake of a particular ligand or metal is observed. For example, use of a 1:1 mixture of H_2bdc and 1,4-H_2ndc in the reaction with zinc(II) nitrate gave $[Zn_4O(bdc)_{1.97}(1,4\text{-}ndc)_{1.03}]$ **113**.[11] This differential uptake of linkers is not well understood, and needs further study. While steric considerations are likely to influence uptake, they cannot be the only factor involved, since a 1:1 mixture of H_2bdc and H_2bdc-Me_2 reacted with zinc(II) nitrate to give $[Zn_4O(bdc)_{1.34}(bdc\text{-}Me_2)_{1.66}]$ **114**, with greater uptake of the bulkier dicarboxylate, whereas use of the approximately isosteric acids H_2bpdc-CHO and H_2bpdc-OMe with zinc(II) nitrate gave $[Zn_4O(bpdc\text{-}CHO)_{0.3}(bpdc\text{-}OMe)_{2.7}]$ **9**.[19]

Examples of cases in which MC-MOFs have properties that are enhanced over their single-ligand or single-metal analogues are given in Table 1.

*** Table 1 here ***

Control of the proportions of ligands or metals in a MC-MOF is important, as this can allow optimisation of a particular property. For example, Rosseinsky and co-workers showed that

$[Cu_3(btc)_2(map)_{1.8}(H_2O)_{1.2}]$ **74a** adsorbs NO reversibly, converting the secondary amine into an *N*-diazenium diolate, whereas this reaction did not occur with either higher or lower loadings of map into $[Cu_3(btc)_2(H_2O)_3]$ **73**.[56] As another example, control of the Tb/Eu ratio in mixed-lanthanide MOFs provides a means to control the colour of the photoluminescent emissions.[73]

MC-MOFs in which different ligands play the same structural role, formed either through direct synthesis or post-synthetic modification, contain pores with a greater degree of complexity than is possible in MOFs that possess a single type of linker. While complete control of the pore structure is not yet possible, an element of tuning does exist, and this has been used to enhance the properties of the resultant product. So, for example, $[Zn_2(bdc)(tmbdc)(dabco)]$ **7** shows a higher degree of hydrogen adsorption than either $[Zn_2(bdc)_2(dabco)]$ **1** or $[Zn_2(tmbdc)_2(dabco)]$ **8**.[18] Mixed-ligand MC-MOFs can show properties of both parent compounds, as witnessed by the combination of CO_2 uptake and selectivity displayed by $[Zn(1,3\text{-bdc-}NO_2)_{0.13}(1,3\text{-bdc-OMe})_{0.87}(4,4'\text{-bipy})]$ **22b**.[21] In addition, surface-modification has been shown to lead to changes in physical properties such as hydrophilicity/hydrophobicity, which in turn can affect chemical stability to moisture.

MC-MOFs can display properties that are not simply the linear combinations of those of the parent MOFs. For example, $[Zn_4O(bdc\text{-}NO_2)_{0.74}\{bdc\text{-}(OAl)_2\}_{1.06}\{bdc\text{-}(OBz)_2\}_{1.20}]$ **19** shows considerably better selectivity for adsorbing CO_2 over CO than MOF-5.[11] This may imply the presence of distinct sequences of linkers within the MC-MOF frameworks, suggesting some MC-MOFs may be more structurally complex than simple solid solutions. Indeed, there is likely to be a spectrum of possible structural types with solid solutions, containing complete mixing of the ligands or metals, at one extreme and core-shell MOFs, with complete segregation of the metals or ligands, at the other. While the 'mid-spectrum' materials may be difficult to study at the molecular level, the observation of synergic relationships demonstrates the great potential that MC-MOFs have to display new or enhanced properties. These materials are therefore likely to become an important part of MOF chemistry over the next few years.

Table 1 – Examples of enhanced functionality of MC-MOFs over single-ligand or single-metal analogues.

MC-MOF	Property	Ref.
$[Zn_2(bdc)(tmbdc)(dabco)]$ **7**	Enhanced H_2 adsorption over $[Zn_2(bdc)_2(dabco)]$ **1** and $[Zn_2(tmbdc)_2(dabco)]$ **8**.	18
$[Zn_4O(bdc)_{1.52}\{bdc\text{-}(OAl)_2\}_{0.73}\{bdc\text{-}(OBz)_2\}_{0.76}]$ **16**	Enhanced H_2 uptake over $[Zn_4O(bdc)_{2.05}\{bdc\text{-}(OAl)_2\}_{0.95}]$ **17**, $[Zn_4O(bdc)_{2.14}\{bdc\text{-}(OBz)_2\}_{0.86}]$ **18** and MOF-5	11
$[Zn(1,3\text{-}bdc\text{-}NO_2)_{0.13}(1,3\text{-}bdc\text{-}OMe)_{0.87}(4,4'\text{-}bipy)]$ **22b**	Adsorbs almost as much CO_2 as $[Zn(1,3\text{-}bdc\text{-}OMe)(4,4'\text{-}bipy)]$ **21** but with better selectivity versus CH_4.	22
$[Al(OH)(bdc\text{-}NH_2)_{0.83}\{bdc\text{-}NHCO(CH_2)_6Me\}_{0.17}]$ **53b**	Enhanced hydrophobicity over $[Al(OH)(bdc\text{-}NH_2)]$ **52**	46
$[Cu_3(btc)_2(map)_{1.8}(H_2O)_{1.2}]$ **74a**	Enhanced NO adsorption over analogues with higher or lower map content.	56
$[EuTb(adipate)_3(H_2O)_2]\cdot$4,4'-bipy **87**	Enhanced Eu^{3+} emission over analogue with no terbium.	69
$[Tb(btc)(H_2O)]\cdot 3H_2O$ **92** doped with Eu^{3+}	Change of photoluminescence colour with increasing proportion of Eu^{3+}.	73

References

1. J. L. C. Rowsell and O. M. Yaghi, *Micropor. Mesopor. Mat.*, 2004, **73**, 3.
2. G. Férey, *Chem. Soc. Rev.*, 2008, **37**, 191.
3. R. Robson, *Dalton Trans.*, 2008, 5113.
4. S. Horike, S. Shimomura and S. Kitagawa, *Nature Chem.*, 2009, **1**, 695.
5. A. U. Czaja, N. Trukhan and U. Müller, *Chem. Soc. Rev.*, 2009, **38**, 1284.
6. L. J. Murray, M. Dincă and J. R. Long, *Chem. Soc. Rev.*, 2009, **38**, 1294.
7. J.-R. Li, R. J. Kuppler and H.-C. Zhou, *Chem. Soc. Rev.*, 2009, **38**, 1477.
8. L. Ma, C. Abney and W. Lin, *Chem. Soc. Rev.*, 2009, **38**, 1248.
9. D. J. Tranchemontagne, J. L. Mendoza-Cortés, M O'Keeffe and O. M. Yaghi, *Chem. Soc. Rev.*, 2009, **38**, 1257.
10. W. Kleist, F. Jutz, M. Maciejewski and A. Baiker, *Eur. J. Inorg. Chem.*, 2009, 3552.
11. H. Deng, C. J. Doonan, H. Furukawa, R. B. Ferreira, J. Towne, C. B. Knobler, B. Wang and O. M. Yaghi, *Science*, 2010, **327**, 846.
12. K. Koh, A. G. Wong-Foy and A. J. Matzger, *Chem. Commun.*, 2009, 6162.
13. D. N. Dybtsev, H. Chun and K. Kim, *Angew. Chem. Int. Ed.*, 2004, **43**, 5033.
14. K. Koh, A. G. Wong-Foy and A. J. Matzger, *Angew. Chem. Int. Ed.*, 2008, **47**, 677.
15. K. Koh, A. G. Wong-Foy and A. J. Matzger, *J. Am. Chem. Soc.*, 2010, **132**, 15005.
16. A. D. Burrows, C. G. Frost, M. F. Mahon, P. R. Raithby, C. L. Renouf, C. Richardson and A. J. Stevenson, *Chem. Commun.*, 2010, **46**, 5067.
17. S. R. Caskey and A. J. Matzger, *Inorg. Chem.*, 2008, **47**, 7942.
18. H. Chun, D. N. Dybtsev, H. Kim and K. Kim, *Chem. Eur. J.*, 2005, **11**, 3521.
19. A. D. Burrows, C. G. Frost, M. F. Mahon and C. Richardson, *Angew. Chem. Int. Ed.*, 2008, **47**, 8482.
20. W. Kleist, M. Maciejewski and A. Baiker, *Thermochim. Acta*, 2010, **499**, 71.
21. T. Fukushima, S. Horike, Y. Inubushi, K. Nakagawa, Y. Kubota, M. Takata and S. Kitagawa, *Angew. Chem. Int. Ed.*, 2010, **49**, 4820.
22. K. M. L. Taylor-Pashow, J. Della Rocca, Z. Xie, S. Tran and W. Lin, *J. Am. Chem. Soc.*, 2009, **131**, 14261.
23. S. Marx, W. Kleist, J. Huang, M. Maciejewski and A. Baiker, *Dalton Trans.*, 2010, **39**, 3795.
24. K. S. Park, Z. Ni, A. P. Côté, J. Y. Choi, R. Huang, F. J. Uribe-Romo, H. K. Chae, M. O'Keeffe and O. M. Yaghi, *Proc. Nat. Acad. Sci. USA*, 2006, **103**, 10186.
25. R. Banerjee, A. Phan, B. Wang, C. Knobler, H. Furukawa, M. O'Keeffe and O. M. Yaghi, *Science*, 2008, **319**, 939.
26. R. Banerjee, H. Furukawa, D. Britt, C. Knobler, M. O'Keeffe and O. M. Yaghi, *J. Am. Chem. Soc.*, 2009, **131**, 3875.
27. T. Wu, X. Bu, J. Zhang and P. Feng, *Chem. Mater.*, 2008, **20**, 7377.

28. S. S. Han, J. L. Mendoza-Cortés and W. A. Goddard III, *Chem. Soc. Rev.*, 2009, **38**, 1460.

29. K. L. Mulfort and J. T. Hupp, *J. Am. Chem. Soc.*, 2007, **129**, 9604.

30. K. L. Mulfort and J. T. Hupp, *Inorg. Chem.*, 2008, **47**, 7936.

31. K. L. Mulfort, T. M. Wilson, M. R. Wasielewski and J. T. Hupp, *Langmuir*, 2009, **25**, 503.

32. Z. Wang and S. M. Cohen, *Chem. Soc. Rev.*, 2009, **38**, 1315.

33. Z. Wang and S. M. Cohen, *J. Am. Chem. Soc.*, 2007, **129**, 12368.

34. K. K. Tanabe, Z. Wang and S. M. Cohen, *J. Am. Chem. Soc.*, 2008, **130**, 8508.

35. Z. Wang and S. M. Cohen, *Angew. Chem. Int. Ed.*, 2008, **47**, 4699.

36. Z. Wang, K. K. Tanabe and S. M. Cohen, *Chem. Eur. J.*, 2010, **16**, 212.

37. J. S. Costa, P. Gamez, C. A. Black, O. Roubeau, S. J. Teat and J. Reedijk, *Eur. J. Inorg. Chem.*, 2008, 1551.

38. E. Dugan, Z. Wang, M. Okamura, A. Medina and S. M. Cohen, *Chem. Commun.*, 2008, 3366.

39. S. J. Garibay, Z. Wang, K. K. Tanabe and S. M. Cohen, *Inorg. Chem.*, 2009, **48**, 7341.

40. D. Britt, C. Lee, F. J. Uribe-Romo, H. Furukawa and O. M. Yaghi, *Inorg. Chem.*, 2010, **49**, 6387.

41. M. J. Ingleson, J. Perez Barrio, J.-B. Guilbaud, Y. Z. Khimyak and M. J. Rosseinsky, *Chem. Commun.*, 2008, 2680.

42. X. Zhang, F. X. Llabrés i Xamena and A. Corma, *J. Catal.*, 2009, **265**, 155.

43. Z. Wang, K. K. Tanabe and S. M. Cohen, *Inorg. Chem.*, 2009, **48**, 296.

44. K. K. Tanabe and S. M. Cohen, *Angew. Chem. Int. Ed.*, 2009, **48**, 7424.

45. K. K. Tanabe and S. M. Cohen, *Inorg. Chem.*, 2010, **49**, 6766.

46. T. Loiseau, C. Serre, C. Huguenard, G. Fink, F. Taulelle, M. Henry, T. Bataille and G. Férey, *Chem. Eur. J.*, 2004, **10**, 1373.

47. J. G. Nguyen and S. M. Cohen, *J. Am. Chem. Soc.*, 2010, **132**, 4560.

48. C. Volkringer and S. M. Cohen, *Angew. Chem. Int. Ed.*, 2010, **49**, 4644.

49. S. C. Jones and C. A. Bauer, *J. Am. Chem. Soc.*, 2009, **131**, 12516.

50. A. D. Burrows, C. G. Frost, M. F. Mahon and C. Richardson, *Chem. Commun.*, 2009, 4218.

51. W. Morris, C. J. Doonan, H. Furukawa, R. Banerjee and O. M. Yaghi, *J. Am. Chem. Soc.*, 2008, **130**, 12626.

52. H. Sato, R. Matsuda, K. Sugimoto, M. Takata and S. Kitagawa, *Nature Mater.*, 2010, **9**, 661.

53. C.-D. Wu, A. Hu, L. Zhang and W. Lin, *J. Am. Chem. Soc.*, 2005, **127**, 8940.

54. S. M. Cohen, *Chem. Sci.*, 2010, **1**, 32.

55. M. Banerjee, S. Das, M. Yoon, H. J. Choi, M. H. Hyun, S. M. Park, G. Seo and K. Kim, *J. Am. Chem. Soc.*, 2009, **131**, 7524.

56. M. J. Ingleson, R. Heck, J. A. Gould and M. J. Rosseinsky, *Inorg. Chem.*, 2009, **48**, 9986.

57. J. G. Nguyen, K. K. Tanabe and S. M. Cohen, *CrystEngComm*, 2010, **12**, 2335.

58. D. Vujovic, H. G. Raubenheimer and L. R. Nassimbeni, *Eur. J. Inorg. Chem.*, 2004, 2943.

59. M.-H. Zeng, B. Wang, X.-Y. Wang, W.-X. Zhang, X.-M. Chen and S. Gao, *Inorg. Chem.*, 2006, **45**, 7069.

60. D. M. Schubert, M. Z. Visi and C. B. Knobler, *Main Group Chem.*, 2008, **7**, 311.

61. M. Fuentes-Cabrera, D. M. Nicholson, B. G. Sumpter and M. Widom, *J Chem. Phys.*, 2005, **123**, 124713.

62. J. A. Botas, G. Calleja, M. Sánchez-Sánchez and M. G. Orcajo, *Langmuir*, 2010, **26**, 5300.

63. W.-C. Song, J.-R. Li, P.-C. Song, Y. Tao, Q. Yu, X.-L. Tong and X.-H. Bu, *Inorg. Chem.*, 2009, **48**, 3792.

64. R. Baggio, M. T. Garland and M. Perec, *Inorg. Chim. Acta*, 1998, **281**, 18.

65. C. Serre, F. Millange, C. Thouvenot, N. Gardant, F. Pellé and G. Férey, *J. Mater. Chem.*, 2004, **14**, 1540.

66. Z.-H. Cai, Y. Tang, W.-S. Liu and M.-Y. Tan, *Chem. Lett.*, 2004, **33**, 342.

67. D. Sendor, M. Hilder, T. Juestel, P. C. Junk and U. H. Kynast, *New J. Chem.*, 2003, **27**, 1070.

68. D. Sarma, M. Prabu, S. Biju, M. L. P. Reddy and S. Natarajan, *Eur. J. Inorg. Chem.*, 2010, 3813.

69. D. T. de Lill, A. de Bettencourt-Dias and C. L. Cahill, *Inorg. Chem.*, 2007, **46**, 3960.

70. P. C. R. Soares-Santos, L. Cunha-Silva, F. A. Almeida Paz, R. A. Sá Ferreira, J. Rocha, T. Trindade, L. D. Carlos and H. I. S. Nogueira, *Cryst. Growth Des.*, 2008, **8**, 2505.

71. A. Thirumurugan and A. K. Cheetham, *Eur. J. Inorg. Chem.*, 2010, 3823.

72. K. Liu, G. Jia, Y. Zheng, Y. Song, M. Yang, Y. Huang, L. Zhang and H. You, *Inorg. Chem. Commun.*, 2009, **12**, 1246.

73. K. Liu, H. You, Y. Zheng, G. Jia, Y. Song, Y. Huang, M. Yang, J. Jia, N. Guo and H. Zhang, *J. Mater. Chem.*, 2010, **20**, 3272.

74. K. A. White, D. A. Chengelis, K. A. Gogick, J. Stehman, N. L. Rosi and S. Petoud, *J. Am. Chem. Soc.*, 2009, **131**, 18069.

75. K. A. White, D. A. Chengelis, M. Zeller, S. J. Geib, J. Szakos, S. Petoud and N. L. Rosi, *Chem. Commun.*, 2009, 4506.

76. S. Das, H. Kim and K. Kim, *J. Am. Chem. Soc.*, 2009, **131**, 3814.

77. G. Férey, F. Millange, M. Morcrette, C. Serre, M.-L. Doublet, J.-M. Grenèche and J.-M. Tarascon, *Angew. Chem. Int. Ed.*, 2007, **46**, 3259.

78. C. Combelles, M. B. Yahia, L. Pedesseau and M.-L. Doublet, *J. Phys. Chem. C*, 2010, **114**, 9518.

79. L. Xie, S. Liu, C. Gao, R. Cao, J. Cao, C. Sun and Z. Su, *Inorg. Chem.*, 2007, **46**, 7782.

80. J. H. Yoon, S. B. Choi, Y. J. Oh, M. J. Seo, Y. H. Jhon, T.-B. Lee, D. Kim, S. H. Choi and J. Kim, *Catal. Today*, 2007, **120**, 324.

81. Y.-Z. Zheng, W. Xue, W.-X. Zhang, M.-L. Tong, X.-M. Chen, F. Grandjean, G. J. Long, S.-W. Ng, P. Panissod and M. Drillon, *Inorg. Chem.*, 2009, **48**, 2028.

82. P. Amo-Ochoa, L. Welte, R. González-Prieto, P. J. Sanz Miguel, C. J. Gómez-García, E. Mateo-Martí, S. Delgado, J. Gómez-Herrero and F. Zamora, *Chem. Commun.*, 2010, **46**, 3262.

83. M. Meilikhov, K. Yusenko, A. Torrisi, B. Jee, C. Mellot-Draznieks, A. Pöppl and R. A. Fischer, *Angew. Chem. Int. Ed.*, 2010, **49**, 6212.

84. S. Furukawa, K. Hirai, K. Nakagawa, Y. Takashima, R. Matsuda, T. Tsuruoka, M. Kondo, R. Haruki, D. Tanaka, H. Sakamoto, S. Shimomura, O. Sakata and S. Kitagawa, *Angew. Chem. Int. Ed.*, 2009, **48**, 1766.

85. Y. Yoo and H.-K. Jeong, *Cryst. Growth Des.*, 2010, **10**, 1283.

86. S. Furukawa, K. Hirai, Y. Takashima, K. Nakagawa, M. Kondo, T. Tsuruoka, O. Sakata and S. Kitagawa, *Chem. Commun.*, 2009, 5097.

87. T. Gadzikwa, G. Lu, C. L. Stern, S. R. Wilson, J. T. Hupp and S. T. Nguyen, *Chem. Commun.*, 2008, 5493.

88. T. Gadzikwa, O. K. Farha, C. D. Malliakas, M. G. Kanatzidis, J. T. Hupp and S. T. Nguyen, *J. Am. Chem. Soc.*, 2009, **131**, 13613.

89. M. Kondo, S. Furukawa, K. Hirai and S. Kitagawa, *Angew. Chem. Int. Ed.*, 2010, **49**, 5327

90. W. J. Rieter, K. M. L. Taylor and W. Lin, *J. Am. Chem. Soc.*, 2007, **129**, 9852.